Journal of Hydrology: Regional Studies 59 (2025) 102414

Contents lists available at ScienceDirect

Journal of Hydrology: Regional Studies

journal homepage: www.elsevier.com/locate/ejrh

Unraveling agricultural water use in three Central Asian irrigation oases using remote sensing

Silvan Ragettli [a], Adrian Kreiner [a,b,*], Andrey Yakovlev [a], Oyture Anarbekov [c], Maha Al-Zu'bi [d], Abdikhamid Urazkeldiyev [e], Tobias Siegfried [a]

[a] hydrosolutions GmbH, Venusstrasse 29, Zürich CH-8050, Switzerland
[b] European Space Agency, Frascati, Italy
[c] Caritas Switzerland in Uzbekistan, Samarkand, Uzbekistan
[d] International Water Management Institute, MENA Office, Giza 12513, Egypt
[e] Hydro Tech Consulting, Shymkent, Kazakhstan

ARTICLE INFO

Keywords:
Integrated water resource management
Remote sensing
Central asia
Irrigation water demand
Water storage

ABSTRACT

Study Region: Three major irrigation oases in Uzbekistan (Bukhara, Samarkand and Kashkadarya)
Study focus: The study employs remote sensing to develop enhanced methodologies for quantifying water use in Central Asian irrigation oases from 2017 to 2022. By integrating earth observation data into a water balance approach, we quantify variables that are typically challenging to measure, such as groundwater overdraft and non-growing season water use for soil preparation. A key aspect of agricultural water management in the region is utilizing water from reservoirs. Here we introduce a novel approach that combines optical remote sensing with satellite laser altimetry to monitor the availability and use of active water storage in reservoirs.
New hydrological insights for the region: Results indicate that water from reservoir storage satisfies up to 14.9 % ± 2.2 % of the annual demand, but another 11.5 % ± 5.2 % are groundwater withdrawals. Our analysis indicates a necessary average annual reduction in groundwater extractions by at least 8.0 % ± 1.6 % for sustainability. Additionally, highly energy-intensive water pumping from Amu Darya River provides more than half of the water resources used in Bukhara and Kashkadarya, resulting in a significant carbon footprint of the region's agricultural production. The detailed breakdown of water uses and irrigation water consumption by crop type informs efficient, sustainable water management, offering new opportunities for agricultural water accounting in Central Asian irrigation oases.

1. Introduction

The Earth's drylands face significant challenges in sustainable water management (Mishra et al., 2021; Stringer et al., 2021). In many places, a major contributor to these challenges is the intensive and inefficient water use for agriculture (Grafton et al., 2018; Scanlon et al., 2023). In Central Asia (CA) irrigated agriculture is prevalent and accounts for approximately 90 % of the region's

* Corresponding author at: hydrosolutions GmbH, Venusstrasse 29, Zürich CH 8050, Switzerland.
E-mail addresses: ragettli@hydrosolutions.ch (S. Ragettli), kreiner@hydrosolutions.ch (A. Kreiner), yakovlev@hyrosolutions.ch (A. Yakovlev), oanarbekov@caritas.ch (O. Anarbekov), m.al-zubi@cgiar.org (M. Al-Zu'bi), urazkeldiev@mail.ru (A. Urazkeldiyev), siegfried@hydrosolutions.ch (T. Siegfried).

https://doi.org/10.1016/j.ejrh.2025.102414
Received 28 June 2024; Received in revised form 8 April 2025; Accepted 20 April 2025
Available online 28 April 2025
2214-5818/

freshwater use (Frenken, 2013; Rakhmatullaev et al., 2013). Given the necessity for irrigation across most of CA, water is by far the most critical factor driving the economic and social development in the region (Li et al., 2020). Historically, agricultural water use in the region has been marked by inefficiencies (Aleksandrova et al., 2014), characterized by both inefficient irrigation methods (Bekchanov et al., 2010, 2014) and significant conveyance losses (Bekchanov, 2024) due to outdated and poorly maintained irrigation canal infrastructures. Inefficient use of water has led to the ongoing decrease in terrestrial water storage (Z. Hu et al., 2021; Yang et al., 2021). Groundwater overexploitation is a widespread problem in irrigation oases, especially where there is heavy reliance on groundwater to offset the irregular availability of surface water resources (Hashemy Shahdany et al., 2018). Waterlogging and soil salinization (Qadir et al., 2009), and energy-intensive water pumping (Djumaboev et al., 2019) are further straining fragile water resources. Recent studies have shown the importance of improving water strategies (Conrad et al., 2020), suggesting that investments in irrigation infrastructure can significantly reduce water use and increase efficiency (Bekchanov et al., 2016; Törnqvist and Jarsjö, 2012).

Sustainable management of freshwater resources begins with precise estimates of irrigation water withdrawals (Patle et al., 2023). Conducting a water balance analysis is essential for identifying and quantifying water fluxes (Cunha et al., 2019; Taghvaeian and Neale, 2011). Yet, the limited availability of reliable agricultural monitoring data in Central Asia challenges this process. Remote sensing can support sustainable development in data-poor regions by supplying complementary data to in-situ monitoring networks (Sheffield et al., 2018). Its techniques are increasingly used as alternatives for water quantification at various scales, providing essential data on terrestrial water storage (Cai et al., 2016; Donchyts et al., 2022; Ragettli et al., 2022; Yao et al., 2023), cropped and irrigated areas (Ragettli et al., 2018; Xiong et al., 2017), as well as crop and irrigation water demand and usage (Foster et al., 2020; Fuentes et al., 2024; Msigwa et al., 2021; Zhang et al., 2022). Despite advances in remote sensing applications for water balance studies, most approaches have focused on individual components, such as evapotranspiration monitoring (Conrad et al., 2013; Hao et al., 2023), seasonal water changes (Che et al., 2019; Klein et al., 2014; Liu et al., 2019) or groundwater depletion tracking (Z. Hu et al., 2019). However, these studies often lack integration of multiple water sources into a unified framework.

While research has examined groundwater reliance in irrigation oases (Awan et al., 2016; Ibrakhimov et al., 2018) or the role of reservoirs in irrigation supply (Biemans et al., 2011; Schmitt and Rosa, 2024), few studies have systematically combined these elements to provide a full accounting of irrigation water sources. A recent water storage change assessment using GRACE-based Terrestrial Water Storage (TWS) estimates (Gafurov et al., 2024) has provided valuable insights into large-scale seasonal water

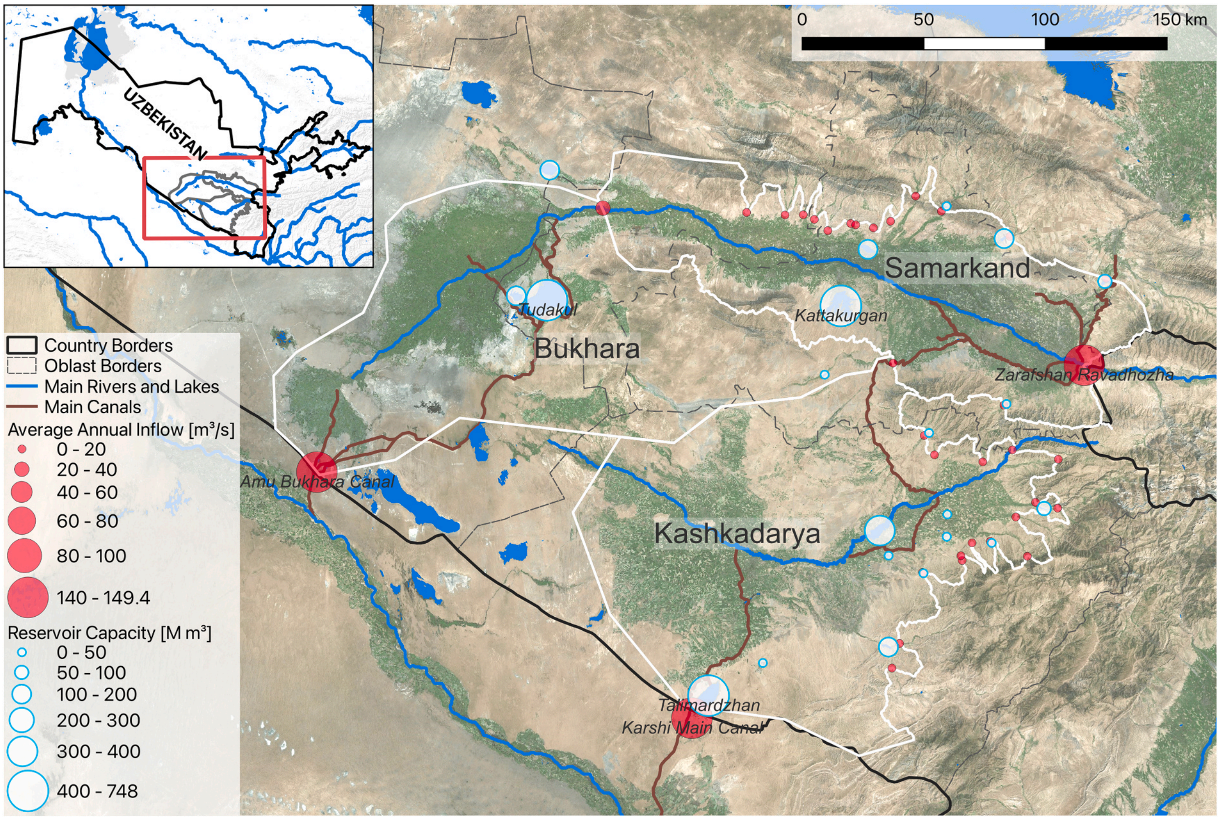

Fig. 1. The study area with the three defined subregions (white outlines): Bukhara, Kashkadarya, and Samarkand oasis. The map highlights the key hydrological features of the area, including reservoirs and the three primary river or canal inflows. Each reservoir is marked with a point, scaled proportionally to its storage capacity in million cubic meters (M m^3), and each inflow point is similarly scaled according to its mean annual rate in cubic meters per second (m^3/s). The background satellite imagery is provided by Bing Aerial. The canal system was obtained from OpenStreetMap.

redistribution in Central Asia, and has shown the importance of regional natural and irrigation-induced water transport processes. However, existing approaches for analyzing the water balance of irrigated areas still lack sufficient data to unravel agricultural water use and its sources at the seasonal and sub-seasonal scales. In particular, the role of seasonal surface water storage in meeting crop-specific water needs is not well understood, especially in terms of its interaction with groundwater extraction. Water balance models struggle to distinguish the use of storage from local aquifers and reservoirs without knowledge of reservoir operating rules (Garcia et al., 2020).

This study formulates a comprehensive method for analyzing the agricultural water balance in Central Asia, incorporating enhanced remote sensing techniques specially designed to address the challenges of understanding water sources for irrigation. The focus is on three irrigation oases — Samarkand, Bukhara, and Kashkadarya — located in Uzbekistan, within the Zarafshan-Kashkadarya River Basin (ZKRB). This transboundary region, shared by Tajikistan and Uzbekistan, is known for its intensive irrigation agriculture. Based on remote sensing and reanalysis data we estimate evaporation from reservoirs, map irrigated areas and major crop types, identify cropping periods, quantify actual evapotranspiration, and calculate crop irrigation water consumption. The datasets are combined with discharge data to unravel the monthly and annual water balance characteristics of the three irrigation oases from 2017 to 2022. The residuals in the water balance are attributed to variables that are challenging to measure, such as groundwater use, and water use during the non-growing season for soil preparation. We analyze seasonal fluctuations in water storage and use and identify periods when groundwater pumping is intensified to supplement other water sources, highlighting times of water scarcity. To improve the accuracy and reliability of our findings, we supplement remote sensing data with on-site measurements for validation. By integrating multiple remote sensing techniques with water balance modeling, this study provides an innovative approach that overcomes the limitations of previous methods that examined only isolated water sources. The goal is to provide enhanced methodologies and tools for decision-makers to quantify and monitor water use. This will offer insights that inform more efficient and sustainable water management practices, contributing to the broader efforts to address water resource challenges in CA and other arid agricultural regions.

2. Study area and climate

The three subregions defined in this study (Bukhara, Samarkand, and Kashkadarya, as shown in Fig. 1) include all irrigated areas within the Zarafshan and the Kashkadarya River Basin located in Uzbekistan. The outlines of the three subregions have been defined using drainage basin boundaries of gauge locations and irrigation oasis boundaries in the lowland areas. The areas of the Bukhara, Samarkand, and Kashkadarya oases are 16,560 km^2, 12,390 km^2, and 15,680 km^2, respectively. The ZKRB is part of the Aral Sea Basin, but due to extensive water withdrawals for irrigation purposes, the rivers have not reached the Amu Darya since the 1960s (Groll et al., 2015a). The elevation of the ZKRB ranges from 5228 m above sea level (m asl) to 176 m asl in its lower regions. The irrigation oases are located below 1100 m asl.

The ZKRB has a typical arid continental climate with cold, dry winters and hot summers. Rainfall occurs mainly in winter and spring; the long-term average annual rainfall amounts to about 240 mm, while potential evapotranspiration exceeds 3000 mm per year (Supplementary Figure A2). The Bukhara oasis experiences the lowest precipitation levels combined with the highest PET compared to other regions.

A majority of the population in rural areas of the study region depends on income from irrigated agriculture (Djumaboev et al., 2017). The main crop-growing period lasts from April to September. Off-season (October – March) irrigation refers to the practice of applying water to agricultural fields during the non-growing season to leach salts from the soil and improve conditions for the subsequent growing season. Inadequate drainage has resulted in widespread waterlogging and secondary soil salinization, affecting roughly half of the land (Hamidov et al., 2016). This negatively affects cotton and wheat production (Varis, 2014). Increasing irrigational water demand in the upstream regions also led to water shortages in downstream regions (Abdullaev, 2004) and deterioration of the water quality (Groll et al., 2015b; Olsson et al., 2013).

The hydrology of the ZKRB is heavily impacted by human activities, including the extensive construction of irrigation canals, lift irrigation schemes and reservoirs. These interventions significantly alter the natural flows of the rivers in the region (Rakhmatullaev et al., 2013). Bukhara and Kashkadarya receive water from the Amu Darya through lift irrigation schemes (Abdullaev, 2004). These schemes have been in service since the mid-1960s, using free, subsidized energy and water (Karimov et al., 2021). The agriculture sector in Uzbekistan accounts for a quarter of the country's electricity consumption (IEA, 2022), whereas the Amu Bukhara Machine Canal is the most extensive pump irrigation system in Uzbekistan, transferring about 4.4 km^3 of water per year to Bukhara Oasis (Karimov et al., 2021). The second connection of the Amu Darya to the ZKRB is through the Karshi Main Canal, which provides water to the Kashkadarya oasis (Fig. 1).

The Zarafshan and Kashkadarya rivers are mainly fed by meltwater from snow and glaciers, resulting in low flows in winter and high flows in spring and early summer (Marti et al., 2023; Olsson et al., 2010). The Eski Ankhor Canal connects the Zarafshan River to the Kashkadarya River and diverts water from the Zarafshan River to the Kashkadarya region (Glovatskii et al., 2023; Glovatsky et al., 2023; Karimov et al., 2021). The Zarafshan River is also connected by the Eski Tuya Tortar Canal to the irrigation network of the Jizzakh Region. This diverts water from the Zarafshan River out of the study area. A schematic visualization of the interlinkages between irrigation schemes, reservoirs, rivers, and canals is provided in Supplementary Figure A1.

In the context of the three study regions, 22 reservoirs have been identified as integral components of water resource management. The Talimardzhan reservoir in the Kashkadarya region is the only off-stream reservoir, meaning it is filled entirely by pumped water rather than natural flow. Tudakul reservoir in Bukhara is partially fed by the Zarafshan River and partially by water pumped from the Amu Darya. Other reservoirs are designed to capture and store water from gravitational flow, which originates from rivers and canals.

3. Data and methods

3.1. Monthly and annual water balance

The water balance approach presented in this study aims at making maximal use of available local measurements, remote sensing and climate reanalysis data to quantify all major components of the monthly and annual water balance of the Bukhara, Samarkand and Kashkadarya oases. The water balance for each oasis is formulated as follows:

$$Q_{in} - Q_{out} + GW - IR_{IS} - IR_{OS} - D - ET_R + R = DS \quad (1)$$

Where Q_{in} is surface water inflow, Q_{out} is surface water outflow, GW is groundwater use, IR_{IS} and IR_{OS} are in- and off-season irrigation water use, respectively, D is domestic water use, ET_R is evaporation from open water surfaces in reservoirs, R represents residuals (unattributed water inputs or uses) and ΔS is the storage change in reservoirs. All variables are expressed in cubic kilometers (km^3) per month (monthly water balance) or km^3 per hydrological year (starting in October and ending in September).

To account for uncertainty in water balance components, we define ranges of plausible values for key variables used in the computation of water balance components (Table 1). While some residuals in the monthly water balance can be attributed to specific processes (Section 3.7), others remain labeled as 'residuals' when their origin is uncertain, thereby allowing the detection of potential measurement uncertainty or unaccounted water sources and uses. While uncertainties exist, the integration of multiple validation strategies for each variable (see Sections 3.2 to 3.7) helps maintain consistency and ensures that estimates remain physically plausible. Fig. 2 provides an overview of the data used, which includes satellite data, field data, and census data.

3.2. Surface water flow

We utilized discharge data from 13 gauges to determine monthly surface water inflow from September 2016 to October 2022. For estimating discharge in 22 smaller, ungauged watersheds, we selected the closest gauged river with a similar watershed area. The monthly runoff modulus calculated for these gauged rivers was then applied to the corresponding ungauged rivers (Shi et al., 2013). Our estimates indicate that the cumulative inflow from these ungauged rivers contributes, on average, only approximately 3.3 % to the total surface water inflow of the study area. All surface water inflow points (gauged and ungauged) are indicated in Fig. 1. A complete list of gauge characteristics is provided in Appendix A by Table A1.

We take the trans-oases fluxes into account properly according to the actual water deliveries. The data from the Navoi gauge on the Zarafshan River serves a dual purpose in our study: it is considered both as an inflow to the Bukhara oasis and as an outflow (denoted as Q_{out} in Eq. 1) from the Samarkand oasis. In contrast, the Bukhara and Kashkadarya oases do not have any river outflow because the Zarafshan and Kashkadarya rivers do not reach the Amu Darya.

To estimate the surface water runoff generated within the irrigation oases, we utilize CHIRPS V2.0 precipitation data (Funk et al., 2015). We consider runoff coefficients ranging from 0.2 to 0.4 (Table 1), to calculate the runoff contribution to the total surface water inflow. This approach allows us to quantify the runoff generated from rainfall within the oases. The runoff coefficients were selected based on local hydrological conditions and historical data (Marti et al., 2023).

3.3. In-season irrigation water use

The calculation of total in-season irrigation water use involves four main steps: i) generation of monthly actual evapotranspiration (ETa) maps for the entire study region and the six-year study period (Section 3.3.1), ii) crop type and irrigated area mapping (Section 3.3.2), iii) identification of the portion of ETa that originates from irrigation (Section 3.3.3) and iv), accounting for the conveyance and field efficiencies to convert actual crop irrigation water use into total in-season irrigation water use (Section 3.3.4).

3.3.1. Evapotranspiration mapping

Daily ETa data for the days of Landsat acquisitions are used in this study to calculate the crop water use (Foley et al., 2023). We use the Landsat Collection 2 Level-3 Provisional Science Product that is publicly available for on-demand processing through the USGS (EROS) ESPA environment (https://espa.cr.usgs.gov/, accessed on 10 January 2024). This product uses the most advanced version of

Table 1
Summary of parameters required for the calculation of water balance components.

Parameter	Unit	Description	Water Balance Component	Mean	Range	Source
E_C	%/100	Conveyance Efficiency	Irrigation Water Use	0.645	0.63–0.66	Kamariddinovich et al. (2023)
E_F	%/100	Field Efficiency	Irrigation Water Use	0.75	0.7–0.8	Conrad et al. (2013)
$E_{F\text{-}OS}$	%/100	Off-Season Field Efficiency	Validation Off-Season Irrigation Water Use	0.2	0.1 – 0.3	Derived from field capacity assumptions (see Appendix B)
RC	%/100	Runoff Coefficient	Surface Water Flow	0.3	0.2–0.4	Marti et al. (2023)
RF	%/100	Reduction factor for irrigation dependence of orchards and trees	Irrigation Water Use	0.63	0.61–0.65	ISMITI (2022)

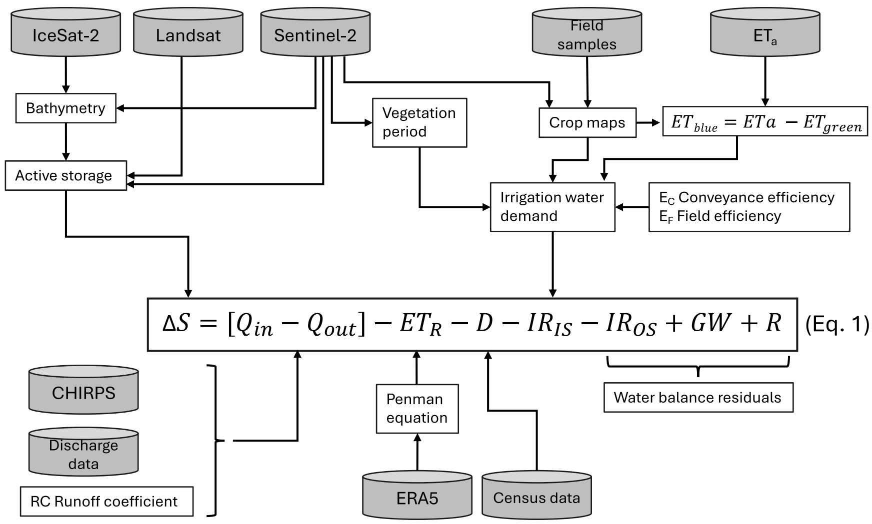

Fig. 2. Workflow diagram illustrating the mass balance calculation integrated with satellite data and field samples.

the Operational Simplified Surface Energy Balance (SSEBop) model (Senay et al., 2023) to retrieve the daily total of ETa (Senay, 2018).

The ETa maps have a spatial resolution of 30 m and were aggregated to a monthly timescale (Pareeth and Karimi, 2023), by averaging all available daily data points. We utilized all available daily ETa layers from Landsat 8 and Landsat 9 and for years up to 2021 we also included all available images from Landsat 7. Given the 16-day revisit interval of each satellite, approximately 3–4 images are available per month throughout the study period. Especially in summer, data availability in the study region is high due to predominantly cloud-free conditions. Supplementary Figure A3 presents a map of the annual ETa for the year 2020.

3.3.2. *Crop type mapping*

We use remote sensing data to provide information on cropped and irrigated areas, crop types, and vegetation periods. The basis for the annual crop maps used in this study are geo-referenced crop type samples collected from 2139 fields in the Kashkadarya region in June 2018 (Remelgado et al., 2020). 930 samples represent cotton fields and 980 samples represent wheat cultivation in single or double crop patterns. In total, the dataset provides samples from five crop cover types (including cotton, wheat, fodder, orchards & vineyards, and double cropping) and one non-crop landcover type (fallow). In addition, 42 samples of non-agricultural irrigated vegetation (e.g., vegetation along irrigation and drainage canals, gardens, and parks), and 35 samples of non-irrigated natural vegetation (e.g., rangeland outside the irrigation oasis) were added manually based on satellite image interpretation. To generate annual crop maps for the 2017–2022 period, we randomly sampled up to 50 pixels from every available crop and land-cover type and used a Random Forest ensemble learning approach for crop type classification (e.g., Tatsumi et al., 2015). We chose to sample only up to 50 samples per class due to the imbalance of available samples between common (cotton, wheat) and uncommon classes (e.g., fodder or double cropping).

The Random Forest classifier is trained on March to October 2018 Sentinel-2 15-day multi-band composites (Normalized Difference Vegetation Index (NDVI), Blue, Green, short wave infrared (SWIR1) and SWIR2 bands) and is subsequently applied to reclassify all pixels for each year 2017–2022 at a resolution of 10 m (Luo et al., 2022). A priori, all pixels labeled by one of the five crop classes are considered irrigated. To avoid misclassifying urban vegetation (such as trees or house gardens) as crops, we utilized the Copernicus Global Land Cover Layers - Collection 2 (Buchhorn et al., 2020) to identify pixels with over 20 % built-up land cover. These pixels, initially labeled as irrigated crops, were reclassified as 'irrigated non-agricultural'.

To obtain monthly maps of irrigated area we perform an analysis of Sentinel-2 15-day NDVI composite images (Pettorelli et al., 2005). Vegetation-rich areas tend to have an NDVI value ranging from 0.3 to 0.8. A time-series analysis of 15-day NDVI allows us to identify the vegetation period. The vegetation period is defined as starting one month prior to NDVI reaching above 0.3 and ends when NDVI drops below this value. Months that fall out of the vegetation period for a given pixel are excluded from the monthly irrigated area maps, which only include pixels labeled as irrigated within their respective vegetation periods.

3.3.3. *Crop Irrigation water use*

The available ETa data is used to estimate green and blue water consumption (Velpuri and Senay, 2017) based on maps of rainfed and irrigated vegetation (Brombacher et al., 2022; Eekelen et al., 2015; Msigwa et al., 2021). Green water is the water stored in the root zone (soil moisture) as the result of precipitation and is equivalent to ETa over rainfed vegetation. ETblue (the portion of ET from irrigation water) is then calculated using the water balance approach (Karimi et al., 2019):

$$ETblue = ETa - ETgreen \tag{2}$$

All variables in Eq. 2 have units of millimeters per month. Eq. 2 is applied to calculate ETblue of all pixels of the monthly crop type maps that are marked as irrigated. ETa in Eq. 2 is actual monthly evapotranspiration per pixel, and ETgreen is average monthly ETa over non-irrigated pixels within the same irrigation oasis, classified as "rangeland" according to the European Space Agency WorldCover 10 m 2020/2021 product (Zanaga et al., 2022). Pixels where monthly ETblue results in a value smaller or equal to zero are reclassified as "non-irrigated".

Ideally, ETgreen is calculated over rainfed agro-ecosystems instead of over rangeland (van Eekelen et al., 2015). However, in the ZKRB, this is not feasible due to the absence of rainfed agriculture within the irrigation oases. Consequently, calculating ETgreen in this context might lead to an underestimation of ETgreen, especially for vegetation types like orchards and trees that can access water from deeper soil layers, unlike the sparser vegetation typically found in rangeland areas. To address this discrepancy and account for the lower irrigation dependence of orchards and trees, which have larger root depths compared to other crops, we have introduced a Reduction Factor (RF, see Table 1).

The rationale behind RF is based on the comparative analysis of irrigation norms for orchards and cotton, the most common crop in the region. This analysis utilized data on recommended irrigation procedures and seasonal irrigation rates for agricultural crops in the Samarkand region (ISMITI, 2022). Our comparison revealed that the irrigation norms for orchards ranged between 68.8 % and 70.7 % of those for cotton. The range of values of RF in this study is calibrated to reflect the same ratio range between average ETblue of cotton and orchards the Samarkand oasis and is then then applied in our water balance approach to adjust ETblue for all orchard and urban vegetation areas. This approach incorporates the reduced irrigation needs of deep-rooted vegetation into our overall estimation of blue water consumption.

3.3.4. *Irrigation efficiency*

ETblue does not account for field application losses nor conveyance efficiencies. To estimate in-season irrigation water use (IR_{IS}) based on actual crop irrigation water use the latter needs to be divided by the conveyance efficiency and by the field efficiency:

$$IR_{IS} = \frac{ETblue * AreaIrrigated}{E_C * E_F} \tag{3}$$

where ETblue (result of Eq. 2, averaged over all irrigated pixels) multiplied by the total irrigated area is monthly actual crop irrigation water use (in m^3 per month), and E_C and E_F are the mean conveyance and field efficiencies, respectively.

Field efficiencies (E_F, see Eq. 1) in Uzbekistan are low due to the widespread furrow irrigation method (Reddy et al., 2013). A field efficiency of 60 % is generally attributed to furrow irrigation (FAO, 1989). However, the actual field efficiency per irrigation oasis in the ZKRB is higher due to the reuse of drainage water (see Appendix B). Conrad et al. (2013) estimated that, on average, 46 % of the freshwater supplied at the system boundaries of the Amu Darya Delta is consumed at the field level. Given a conveyance efficiency (E_C) of 63 %–66 %, this implies a field efficiency of approximately 70 %–80 % ($E_C \times E_F \approx 0.46$). We therefore consider this range of plausible values for E_F (see Table 1). The conveyance efficiency in the Zarafshan River Basin was estimated at 63 % - 66 %, in line with targets set in the Ministry of Water Resources of Uzbekistan's 2021–2023 strategy (Kamariddinovich et al., 2023) and findings from Bekchanov (2024).

3.3.5. *Validation strategy*

Three sources of information are available for validating irrigated area maps and irrigation water use estimates: i) field samples provided by Remelgado et al. (2020) which were not included in the training of the random forest classifier are utilized for an assessment of the accuracy of crop classification in Kashkadarya. The kappa coefficient (Cohen, 1960) and a confusion matrix approach (Foody, 2002) is used to evaluate the crop identification performance. ii) Identified irrigated areas of cotton and wheat are validated against official census data available from Kashkadarya. iii) To validate our estimates of irrigation water use, we use irrigation norms provided by ISMITI (2022). The irrigation norms represent typical irrigation volumes at the farm level, which means that conveyance losses are not accounted for. Therefore, we compare the irrigation norms with our estimates of average annual crop irrigation water use of cotton, fodder, and wheat, divided by E_F.

3.4. *Reservoir storage*

The method to determine the active water storage in reservoirs is based on optical satellite imagery, which is used to observe the position of the water-land boundaries in the reservoirs (Ragettli et al., 2022), and satellite laser altimetry, which is used to derive the bathymetry of reservoirs (Section 3.4.2). Multi-temporal observations of the water-land boundaries in reservoirs enable the derivation of water-level and water volume time series based on the bathymetry of reservoirs (Section 3.4.3).

The surface water occurrence probabilities (SWOP) in lakes and reservoirs can be directly linked to elevation, as the ever-shifting water-land boundaries are identical to elevation contour lines (Mason et al., 1995; Salameh et al., 2019). Previous studies have therefore related multitemporal stacked water occurrence images to elevation information from satellite altimetry, obtaining shallow water bathymetries of water bodies using only satellite data (Armon et al., 2020; Xu et al., 2021). Once the bathymetry is known, the water-land boundary can be matched with elevation information to derive high-accuracy time-series of water levels (Ragettli et al., 2022; Xu et al., 2024). Here we propose a new version of the waterline method to first derive the bathymetry and then the water level changes in reservoirs. The application of the method is ideal for water bodies with strong fluctuations in water level and area. However, by detecting the boundary between water surface and stable terrain along Ice, Cloud, and land Elevation Satellite-2 (ICE-Sat-2) laser tracks our method can also be applied to reservoirs that do not fall dry completely.

3.4.1. Inventory of reservoirs

This study identifies water bodies larger than 1 ha within the study area using the HydroLAKES dataset (Messager et al., 2016) and the ReaLSAT dataset (Khandelwal et al., 2022). In total, 22 reservoirs were identified (Table 2, Fig. 1). Lakes outside the study region (Fig. 1) that are fed by drainage water but do not serve as sources for irrigation or function as water storage facilities for irrigation were not considered.

3.4.2. Reservoir bathymetries

We use Sentinel-2 derived SWOP maps considering all available Sentinel-2 optical images (Level-1C) over all identified reservoirs between October 2017 and September 2022. We chose a five-year period to minimize changes in the bathymetry related to sedimentation processes during the period of analysis while still capturing a representative range of possible water level variations. The Copernicus Sentinel-2 mission acquires multispectral optical imagery at a spatial resolution of 10 m with a revisit time of 5 days (Sentinel-2A and Sentinel-2B).

ICESat-2 is in orbit since September 2018 and has a revisit frequency of 91-days. Equipped with the Advanced Topographic Laser Altimeter System (ATLAS), the satellite measures the time it takes for emitted photons to reflect off the Earth's surface and return. Along the laser track the satellite provides elevation measurements at 0.7 m intervals (Markus et al., 2017). We used all measurements available from the ICESat-2 ATL08 and ATL13 products (Jasinski et al., 2021; Neuenschwander et al., 2021) until October 2022. These two products provide post-processed ground heights at intervals between 5 and 15 m.

A priori it is not known whether the ICESat-2 datapoints represent the elevation of the water surface or ground elevation when the water level is low. We therefore processed all ICESat-2 ground tracks with a changepoint detection algorithm to identify the boundary between the water surface (with equal height) and stable terrain (with decreasing heights for increasing SWOP). To create the relationship between inundation frequency and reservoir bathymetry we fit a monotonically decreasing function to all available data

Table 2
Characteristics of reservoirs used for water resource management in the study region. Water area (in hectares), water level (m asl) and active storage volume (in million m^3) are identified by remote sensing and provide the full range of values identified over the period October 2017 to September 2022. VA-Scaling shape constants (Eq. 4) are used to calculate active storage of those reservoirs for which the bathymetry could not be retrieved. The value in brackets indicates the ID of the reservoir that was used to calculate the shape constants.

ID	Oasis	Name	LON	LAT	Construction Year	Water Area [ha]	Water Level [m asl]	Active Storage [Mm3]	VA-Scaling a, b (Donor ID)
1	Bukhara	Tudakul	64.85	39.85	1979	16012 – 20735	221 – 224.3	34.8 – 651.2	
2	Bukhara	Kuyumazar	64.70	39.87	1960	1001 – 17401	225.7 – 237.9	4.6 – 175.3	
3	Bukhara	Shorkul	64.87	40.33	1984	1401 – 3428	264 – 268.9	1.6 – 107	
4	Bukhara		65.05	40.01		2.4 – 9.2		0.001 – 0.018	2.35E−06, 2.77E+00 (22)
5	Kashkadarya	Talimardzhan*	65.57	38.37	1985	1568 – 5745	371.6 – 391.2	14.9 – 747.8	
6	Kashkadarya	Chimkurgan*	66.40	38.96	1963	112 – 4152	469.5 – 488.5	7.9 – 368.4	
7	Kashkadarya	Pachkamar*	66.42	38.53	1968	91 – 1563	643.9 – 673.6	0.5 – 161.8	
8	Kashkadarya	Hisorak	67.18	39.02		72 – 1150		2.2 – 80.3	8.96E−03, 1.29E+00 (18)
9	Kashkadarya	Kamashi*	66.44	38.87	1987	50 – 362	484.8 – 495.9	0.1 – 22.4	
10	Kashkadarya	Kalkamin	66.65	39.31		6 – 301		0 – 17.7	2.35E−06, 2.77E+00 (22)
11	Kashkadarya	Karabag	66.72	38.93		0.4 – 292		0 – 16.2	2.35E−06, 2.77E+00 (22)
12	Kashkadarya	Uchkizil	66.93	38.90	1957	4.6 – 316	893.4 – 932.3	0.1 – 10.7	
13	Kashkadarya		65.83	38.48		78.5 – 205		0.4 – 6.1	2.35E−06, 2.77E+00 (22)
14	Kashkadarya		66.60	38.80		0 – 190		0 – 4.9	2.35E−06, 2.77E+00 (22)
15	Kashkadarya		66.73	39.01		16 – 81		0.1 – 3	9.34E−05, 2.37E+00 (21)
16	Samarkand	Kattakurgan	66.26	39.80	1968	3010 – 8218	499.4 – 511.1	3.2 – 635.2	
17	Samarkand		67.05	40.02		0 – 962		0 – 128.2	8.96E−03, 1.29E+00 (18)
18	Samarkand	Akdariya	66.40	40.00	1978	252 – 1534	483.5 – 496.3	1.4 – 106.3	
19	Samarkand	Karaultepa	67.53	39.84	1983	0 – 1040	810.2 – 819.9	0.3 – 53.7	
20	Samarkand	Tusunsay	66.78	40.15		66 – 583		0.8 – 49.7	2.93E−04, 1.89E+00 (9)
21	Samarkand	Karatepinskoe	67.03	39.41		16.5 – 330	911.7 – 932.4	0 – 22.9	
22	Samarkand	Kassansay	66.17	39.54		42 – 160	427.2 – 430.1	0 – 3.1	

* Validation data available

points representing stable terrain. Details regarding the changepoint algorithm and the fitted functions are provided in Appendix C.

The bathymetry of the "dead storage" parts of the reservoir that were always underwater between October 2017 and September 2022 cannot be derived. In contrast, the "active storage" part refers to the parts that temporally fall dry towards the end of the irrigation season. If ICESat-2 data for the deepest parts of the active storage zones are not available, the bathymetry of those parts is reconstructed using the extrapolation of the fitted function. This is only done if ICESat-2 data points are available over at least 50 % of the observed SWOP range. Water bodies where this condition cannot be fulfilled are omitted and their volumes will be derived by Area-Volume (AV) scaling (see Section 3.4.3 below). The chances of a successful application of the methodology are higher for larger reservoirs, where more ICESat-2 ground tracks are available. For reservoirs with very steep embankments the algorithm is also likely to fail: the changepoint detection can only be successful for water bodies where the SWOP range stretches over a horizontal distance that exceeds the resolution of the Sentinel-2 imagery and the distance between retrieved ICESat-2 data points.

3.4.3. Active storage changes

With the available bathymetry of the active storage, the elevation of the water-land boundary can be retrieved for any day where optical satellite imagery is available (Ragettli et al., 2022). For this purpose, all satellite images are processed to retrieve binary water-land images (as detailed in Appendix C). Subsequently, a 10 m buffer is added on both sides of the water edge. We sample all bathymetry pixel values at a 10 m resolution within this buffered contour and use the median to calculate a single water surface height (WSH). The procedure is not sensitive to the presence of clouds because the WSH can also be determined if part of the shoreline is not visible. Using the determined WSH in conjunction with the reservoir's geometry, we identify the active storage volume of the reservoirs for any day when optical satellite imagery is available.

We utilized the complete archives of atmospherically corrected surface reflectance images from Landsat 7, Landsat 8, and Landsat 9 (Level 2, Collection 2, Tier 1), as well as all available Sentinel-2 images, to compile time series of reservoir Water Surface Height (WSH) from October 2017 to September 2022 with cloud cover less than 30 %. For each reservoir, monthly active storage volumes are derived by calculating the median of all available data points within the respective month.

As detailed above, the procedure may fail for reservoirs where adequate ICESat-2 data are not available. To determine the storage volume of all reservoirs within the study region, we use Area–Volume (AV) scaling relationships for reservoirs whose bathymetry is unavailable. These relationships are in the form of:

$$V = a * A^b \tag{4}$$

where A is the area, V is the volume of the lake, and a and b are shape constants (Khazaei et al., 2022). The water area of such reservoirs is obtained following the unsupervised method as suggested by Donchyts et al. (2016). The shape constants are then derived from functions fitted to the AV relationship of nearby reservoirs with similar minimum and maximum water areas.

3.4.4. Validation strategy

For validation purposes, we use two types of data available for four reservoirs in Kashkadarya (Table 2): i) time series of decadal total reservoir volume measurements and ii) design information on the maximum available storage and the dead storage of reservoirs. Official data on dead storage volumes are used to adjust the decadal total volume measurements. By subtracting the dead storage volumes from the total, we convert these measurements into active storage values, enabling a validation against our active storage volume estimates. The measured decadal time series are aggregated to monthly time steps.

3.5. Open-water evaporation

The loss of evaporation from the reservoir water storage is calculated based on the Penman equation (e.g., Ragettli et al., 2022; Schulz et al., 2020) with inputs sourced from the ERA5-Land Hourly – ECMWF Climate Reanalysis dataset (Muñoz-Sabater et al., 2021). For specific methodologies applying the Penman equation with ERA5 data, readers are referred to Ragettli et al. (2022).

3.6. Domestic water use

The municipal water usage in the study was estimated using population data from 2017 to 2022, provided by the State Committee of the Republic of Uzbekistan (2023). We assumed a daily water consumption rate of 100 liters per person, as indicated by the Asian Development Bank (ADB, 2016). Due to the lack of specific data on industrial water use and considering the relevant literature (Khaidarov, 2020; Saidmamatov et al., 2020; Wang et al., 2021) we concluded that industrial water consumption within the ZKRB is minimal compared to agricultural usage and thus negligible for this study.

3.7. Groundwater use, off-season irrigation and residuals

In our water balance (Eq. 1), groundwater use and off-season irrigation are the only components without available data. Groundwater is primarily utilized during periods of water scarcity, especially towards the end of the irrigation season when reservoir levels are low and supplies from canal surface water are unreliable. Off-season irrigation, crucial for soil preparation and salt leaching, occurs when there is no visible vegetation response, thus evading detection through evapotranspiration observations. These two components occur in distinct periods: groundwater use during the main irrigation season (May to October) and off-season irrigation outside the main growing season (November to April). Our balance equation attributes positive residuals (water inputs) during the irrigation season to groundwater use and negative residuals (water uses) outside the main growing season to off-season irrigation. Off-season positive residuals and negative residuals during the main irrigation season remain labeled as "residuals" as it is not clear whether they represent unaccounted uses or sources, respectively, or if they are due to measurement uncertainty.

3.7.1. Validation strategy

Total annual groundwater use identified within all three oases is compared to Gravity Recovery and Climate Experiment (GRACE) data (Landerer et al., 2020; Landerer and Swenson, 2012). GRACE is a satellite mission that measures Earth's gravity field variations, which are used to infer changes in mass distribution, including groundwater storage changes. We use the Center for Space Research (CSR) RL06 v02 Mascon Solutions product (Save et al., 2016), providing monthly time series of global mass anomaly grids derived from GRACE observations. From these grids, with a spatial resolution of roughly 120 km, we extracted the mean monthly terrestrial water storage (TWS; units of water equivalent thickness) for the domain defined by the coordinates 40.3°N, 67.5°E, 38.6°S, and 64.1°W (Supplementary Figure A4). Due to the relatively coarse resolution of the data, we did not compare GRACE TWS changes to groundwater use in each individual oasis. Instead, to validate groundwater use, we examined the correlation between annual depletions in TWS and the collective annual groundwater use within all three oases. The depletion in each year is equivalent to the difference between the maximum and the minimum TWS per hydrological year. Missing data points between June 2017 and June 2018 were extrapolated using the multi-annual average storage changes between given months of the year. According to the GRACE TWS data, the maximum TWS is usually reached in April, and the minimum TWS is reached in November each year (Supplementary Figure A4).

Regarding off-season irrigation, two datasets with official data are available: i) the total area treated for salt removal by leaching and off-season water charging, respectively, during the two autumn-winter periods 1998–1999 and 2001–2002, and ii) the annual volume of water drained from the collector-drainage system (years 2019 and 2020). The data are available at the Oblast level. These administrative boundaries only approximately align with the outlines of our defined irrigation oases (Fig. 1). Official data from Navoi Oblast are therefore divided between Bukhara and Samarkand oases according to the relative fraction of irrigated area of each oasis overlapping with Navoi Oblast. The first dataset can only be compared to our results qualitatively, since the validation data specifies the total area where off-season irrigation is applied, while our water balance analysis can only quantify the total volumes of water used. The second dataset can be used for quantitative validation of annual drainage water volumes, but also includes on-season field losses. To validate our results against the official data on total drainage volume, it is necessary to also specify an off-season field efficiency ($E_{F\text{-}OS}$, see Table 1). We estimate that 70 % - 90 % of the water volume used for off-season irrigation will drain through the collector-drainage system. Our assumptions and further details regarding the validation data are specified in Appendix B.

4. Results and discussion

4.1. Monthly and annual water balances

On an annual scale, changes in reservoir storage are insignificant, because reservoirs are practically empty at the end of the

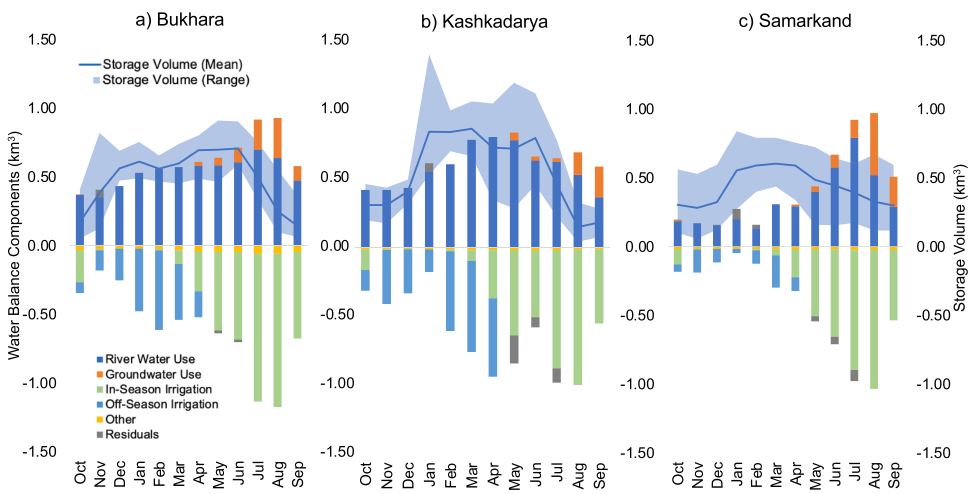

Fig. 3. Monthly water balance components and reservoir storage for the three irrigation oases: a) Bukhara, b) Kashkadarya, and c) Samarkand. The water balance components depicted as stacked bars are groundwater use, river water use ($Q_{in} - Q_{out}$ in Eq. 1), off-season irrigation, in-season irrigation, 'other' (domestic water use and evaporation from reservoirs), and residuals. The components are represented as positive or negative stacked columns depending on their sign in the water balance equation (Eq. 1). Storage changes in reservoirs (ΔS in Eq. 1) are not depicted as stacked columns, but the figure shows the mean monthly total storage volume of reservoirs within each oasis (blue lines). The light blue areas represent the full range of monthly storage volumes observed over the 6 years.

hydrological year (Fig. 3). On a monthly scale, the role of reservoirs as a source of water becomes evident. Reservoirs in Bukhara, Kashkadarya, and Samarkand can store up to 12.5 % ± 1.9 %, 18.8 % ± 3.3 %, and 16.5 % ± 2.4 % of the total annual water inputs. Groundwater use is of similar importance as water from reservoir storage, contributing 11.2 % ± 5.0 %, 6.7 ± 5.1 %, and 18.9 ± 10.5 % to annual water use, respectively.

For Bukhara oasis, the average annual water input was estimated at 7.26 ± 1.1 km^3 , predominantly originating from Amu Darya via the Amu Bukhara Machine Canal (4.71 ± 0.38 km^3, representing 65 % ± 8.0 % of all water inputs there) (Fig. 4, Supplementary Table A2). In terms of water use, agricultural in-season irrigation (water delivered and conveyance loss) was the largest consumer, accounting for 4.67 ± 0.62 km^3 (64.3 % ± 2.6 %) of total water use (Fig. 4, Supplementary Table A2), followed by off-season irrigation (2.09 ± 0.49 km^3, or 28.8 % ± 3.3 % of total water use). 0.38 km^3 ± 0.01 km^3 (5.3 % ± 0.8 %) of water is lost through evaporation from reservoirs. Other water uses, according to our analysis, contribute a negligible percentage to the total water balance.

Similar patterns are observed in Kashkadarya and Samarkand oases (Fig. 4, Supplementary Table A2) with notable variations in the relative importance of individual components such as in- and off-season irrigation water use (results presented below in Sections 4.3 to 4.6). Like Bukhara oasis, Kashkadarya oasis is mainly fed by pumped water from Amu Darya (Karshi Main Canal, providing 4.17 km^3 ± 0.22 km^3, being 55.6 % ± 9.5 % of all water used). In comparison to Bukhara and Kashkadarya, Samarkand is more dependent on natural flows such as inflow through rivers (57.6 % ± 9.2 %) and runoff generated from precipitation (21.3 % ± 6.6 %). Natural flows have a higher inter-annual variability, and it is therefore not surprising that the dependence on groundwater is higher in Samarkand oasis than in Bukhara and Kashkadarya (Fig. 4).

Quantities used to close the annual water balance, which are not specifically attributable to any single component, represent between 0.5 % and 5.1 % of the annual water inputs or water uses, respectively ('residuals', as indicated in Fig. 4). In Bukhara nearly 99 % of the annual water inputs and uses could be attributed to a specific component. This high level of attribution demonstrates a strong correlation between our estimates of total water inputs and total water uses, indicating the robustness of our water balance analysis. At the monthly level, the estimation of monthly reservoir storage changes brings additional uncertainties. However, also in monthly water balances residuals are small. On average they represent only 2.6 % of the monthly water inputs and 1.2 % of the monthly water uses. The largest residuals are present in the water balance for the month of May in Kashkadarya oasis (0.2 km^3, representing 24.5 % of the average total water uses in that month, see Fig. 3b and Supplementary Table A3).

Each major water balance component in each oasis exhibits a characteristic annual cycle, as evidenced by the patterns observed in the monthly water balance components (Fig. 3). Groundwater use peaks in September in Bukhara and Samarkand, and in October in Kashkadarya. Reservoirs in each oasis usually reach capacity levels early in the year, around January or February. In Samarkand, reservoir storage tends to deplete earlier in the season, while water availability from rivers peaks later compared to Bukhara and Kashkadarya. This later peak in Samarkand is largely due to river flows being fed by snow and glacier melt (Marti et al., 2023), which occur later in the year, providing a delayed influx of water. In Bukhara and Kashkadarya, the seasonality of river water use is more uniform due to the continuous pumping of water from Amu Darya. In these two oases, in all months of the year, pumped water represents between 37 % and 84 % of the average monthly water use (Supplementary Table A3).

Despite the differences in the annual cycles of water inputs, the three oases exhibit similar patterns in terms of in-season irrigation

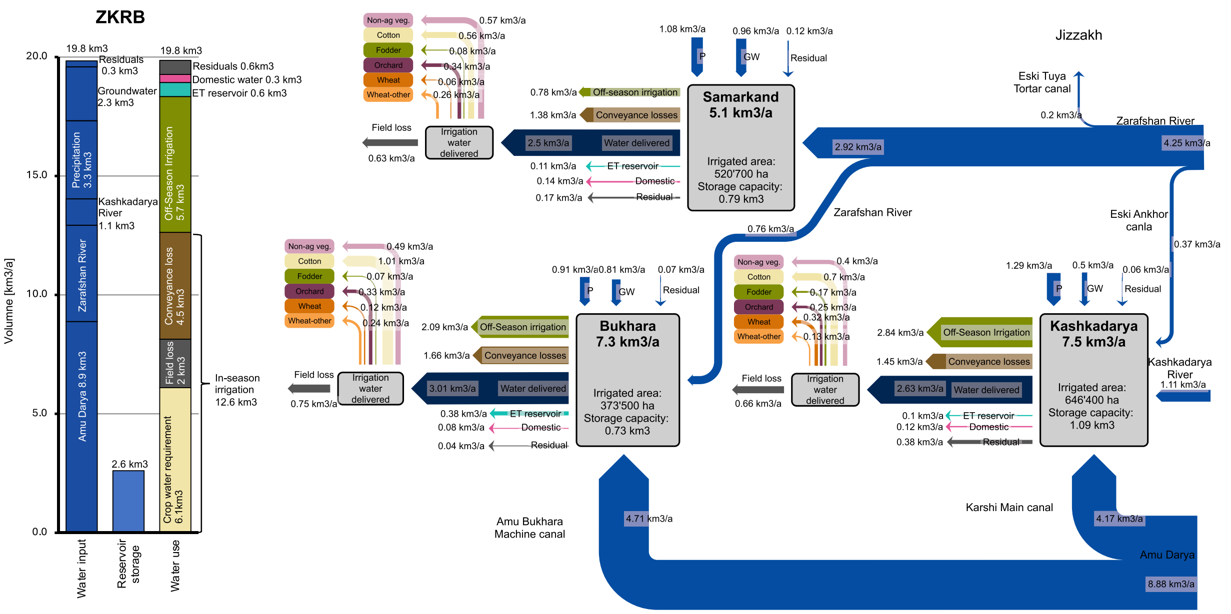

Fig. 4. Sankey diagram of water flows in the ZKRB. The width of the arrows is proportional to the flow rate of the depicted component of the water balance (units of cubic kilometers per year). 'P' represents runoff from precipitation, while 'GW' denotes groundwater use. 'Residuals' refers to quantities used to close the annual water balance, not specifically attributable to any single component.

water use. In all oases, July and August are the months with the highest irrigation water consumption (Fig. 3). A large fraction of the available water in Bukhara and Kashkadarya from November to January is allocated to filling up reservoir storage (up to 72 %, see Supplementary Table A3). However, from February to April, most pumped water is utilized for off-season irrigation. In contrast, losses through off-season irrigation holds much lesser importance in the Samarkand oasis, likely due to drainage water reuse (see Section 4.5).

4.2. Reservoir storage use

According to the remote sensing analysis, the total storage capacity in Bukhara, Kashkadarya and Samarkand is 0.91 km^3, 1.41 km^3, and 0.84 km^3, respectively. Each oasis has one major reservoir, contributing 90 % in Bukhara, 68 % in Kashkadarya, and 65 % in Samarkand to the total storage capacity of each oasis (see Table 2 and labelled reservoirs in Fig. 1). For nine out of 22 reservoirs the storage volumes have been identified based on VA-scaling, because suitable ICESat-2 data were not available to derive their bathymetry. However, this concerns only small reservoirs that represent on average only 2.5 % ± 1.0 % of the total monthly active storage volume in the ZKRB. Detailed results of the bathymetry generation with ICESat-2 data for individual reservoirs are provided in Appendix C.

The yearly active storage capacity aligns well with the measured data (Fig. 5a). Across the four reservoirs, the mean absolute difference in the yearly active storage volume is, on average, only 30.6 %, mainly due to the overestimation of reservoir storage in the Pachkamar reservoir. The total mean yearly active storage volume over the four reservoirs deviates only by 0.2 %. The highest accuracy in estimating active reservoir storage volumes was achieved for the Kamashi and Chimkurgan reservoirs, with mean absolute differences of 0.5 % and 4.6 %. respectively. Conversely, the lowest accuracy was found for the Pachkamar reservoir, with a mean absolute difference of 104 %.

The seasonal variation in monthly active storage (Fig. 5b) is accurately reflected across the reservoirs (Fig. 5b), especially for the largest reservoirs, Talimardzhan and Chimkurgan, with the median of the absolute difference of the monthly change rate equal to 47.6 Mm^3 and 18.6 Mm^3, respectively. These results demonstrate that the active storage reservoir volume changes obtained from remote sensing accurately reflect the monthly use of water from storage.

All large reservoirs in the ZKRB were constructed during the soviet period (Rakhmatullaev et al., 2013; Table 2). The design storage at the year of construction of the reservoirs indicates a substantially higher design storage capacity than what is currently available (Fig. 5a). In the Talimardzhan and Chimkurgan reservoir the design capacity exceeds the actual active storage capacity by more than 80 %. Sedimentation over time, primarily impacting the dead storage of reservoirs, likely has no significant impact on the discrepancies in active storage. The lack of sufficient river water, or the technical conditions of pumping stations in the case of the Talimardzhan reservoir, may explain why reservoirs are not filled to their design storage capacity. Overall, the difference between designed and actual active storage capacity amounts to 0.72 km^3 in Kashkadarya.

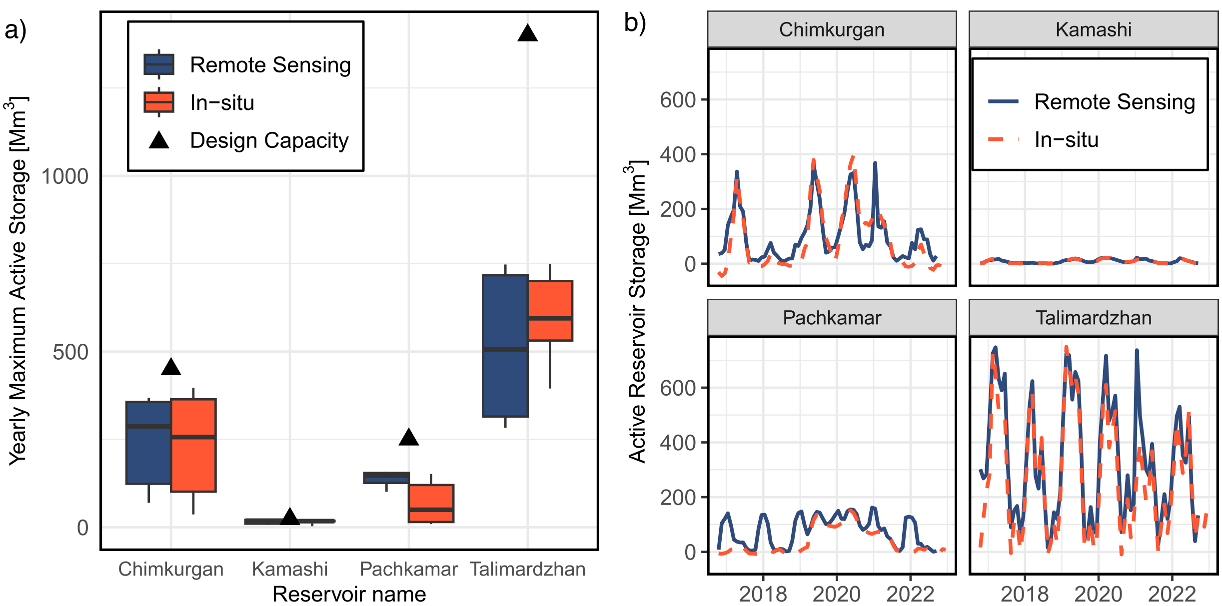

Fig. 5. a) Validation of yearly maximum active storage per reservoir in Kashkadarya Region (2017–2022) against measured in-situ data. The central marks correspond to the median, the edges of each box are the 25th and 75th percentiles and the whiskers extend to the most extreme data points. The black triangles indicate the design capacity of reservoirs at the year of construction. b) Validation of monthly active reservoir storage 2017–2022. Units in million cubic meters (Mm^3).

4.3. Irrigated areas

Cotton and wheat are the two most important crop types in the Kashkadarya oasis (Fig. 6b). By considering only field samples that were not used for the training of the crop classifier, we calculated an overall classification accuracy of 84.5 % (see Supplementary Table A4) and a Kappa statistic of 0.75, indicating high model performance. The producer accuracies for cotton and wheat are 91 % and 80 %, respectively, while the user accuracies are 98.4 % and 99.7 %. The producer accuracy yielded for orchards is 60 % and 78.2 % for fallow areas. For other crop classes, no validation samples are available. Given that only 5 % of the validation samples represent crops other than cotton or wheat, the significant class imbalance has impacted the user accuracies of the less represented classes, resulting in lower figures of 38.1 % and 22.5 % for orchards and fallow areas, respectively. In the Samarkand and Kashkadarya oases, the 'Non-Agricultural' class appears more frequently than the 'Orchards' class (Fig. 6b). However, due to the high risk of misclassifying orchards with trees in house gardens and urban areas, the total area estimates for both the 'Non-Agricultural' and 'Orchards' classes should be interpreted cautiously.

For the validation of total irrigated crop acreages against census data, the 'Non-Agricultural' class is not included. According to our remote sensing analysis, the total annual irrigated cropland area in the Kashkadarya region varied between 370,000 ha and 688,000 ha per year (Fig. 7b). Multi-annual average values align closely with official district data from Kashkadarya province. At the province level, the average annual difference in irrigated cropland area is only 2.5 %, while at the district level, it averages 29.7 %. The wide range of annual irrigated areas is primarily due to significant inter-annual variations in identified wheat growing areas in the Chirakchi and Guzar districts (Fig. 7c), which are not mirrored in the census data. This discrepancy may be due to the census data not being updated annually, as indicated by the minimal year-to-year variations in the official data (Fig. 7b-d). However, the inter-annual variations relative to the total irrigated area are four times larger in Kashkadarya than in Bukhara, and two times larger than in Samarkand (Fig. 6). The inter-annual variations in the Chirakchi and Guzar districts are therefore likely attributable to misclassification of natural vegetation responses in springs with unusually high rainfall. The impact on irrigation water use estimates is however limited, as wheat's contribution to total irrigation water use in the Kashkadarya oasis is only 4.3 % ± 0.5 % (Supplementary Table A2). Accounting for conveyance and field losses, the share of wheat irrigation water use of total water use varies by approximately ± 0.9 %. Cotton areas, which are much more relevant regarding their share of total irrigation water use (9.3 % ± 3.8 % in Kashkadarya oasis, Supplementary Table A2) show a very good agreement with census data (average difference of 2.3 % at the province level and 20.6 % at the district level, see Fig. 7d).

4.4. Irrigation water use

The irrigation norms from Samarkand align well with the estimates from remote sensing. Across all four crop classes for which irrigation norms are available (cotton, fodder, orchards and wheat), the mean absolute difference is on average only 12.5 % (Fig. 8a). The irrigation norms were used to calibrate the irrigation water use of orchards relative to cotton, but the absolute values were not used for calibration. In agreement with the irrigation norms, fodder is the most irrigation intensive crop in Samarkand (7470 ± 500 m^3/ha), followed by cotton (6630 ± 440 m^3/ha). Irrigation water use for orchards, double cropping and irrigated non-agricultural areas is similar, each averaging around 4500 ± 500 m^3/ha. Wheat cultivated as a single annual crop requires in Samarkand almost three times less irrigation water than cotton, and two times less than orchards (2280 ± 150 m^3/ha).

The order of Irrigation intensity per crop class is identical in Bukhara and Kashkadarya, but the absolute irrigation water needs are substantially higher in Bukhara (Supplementary Figure A5). Cotton in Bukhara requires on average 53–58 % more irrigation water than in Kashkadarya or Samarkand. Wheat cultivation in Bukhara even requires more than twice the amount of irrigation than in the two other oases. The differences are caused by the more arid climate in Bukhara, which leads to much higher crop evapotranspiration (Supplementary Figure A3) and irrigation water needs.

The substantially higher crop irrigation water demand of cotton than wheat is in agreement with previous studies from the region

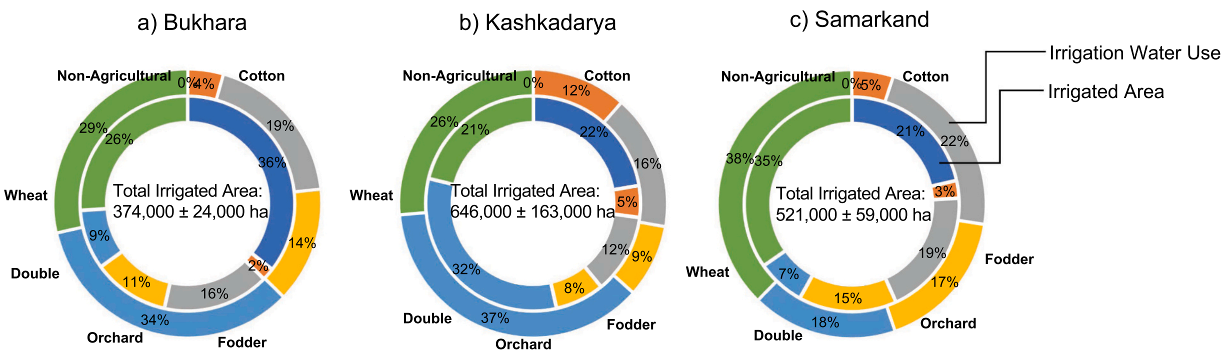

Fig. 6. Fraction of irrigated area (inner ring) and fraction of total irrigation water use (outer ring) per crop class and for each irrigation oasis. 'Double' denominates double cropping (wheat & other), 'Orchards' includes orchards and vineyards, and 'Non-Agricultural' refers to house gardens and urban vegetation.

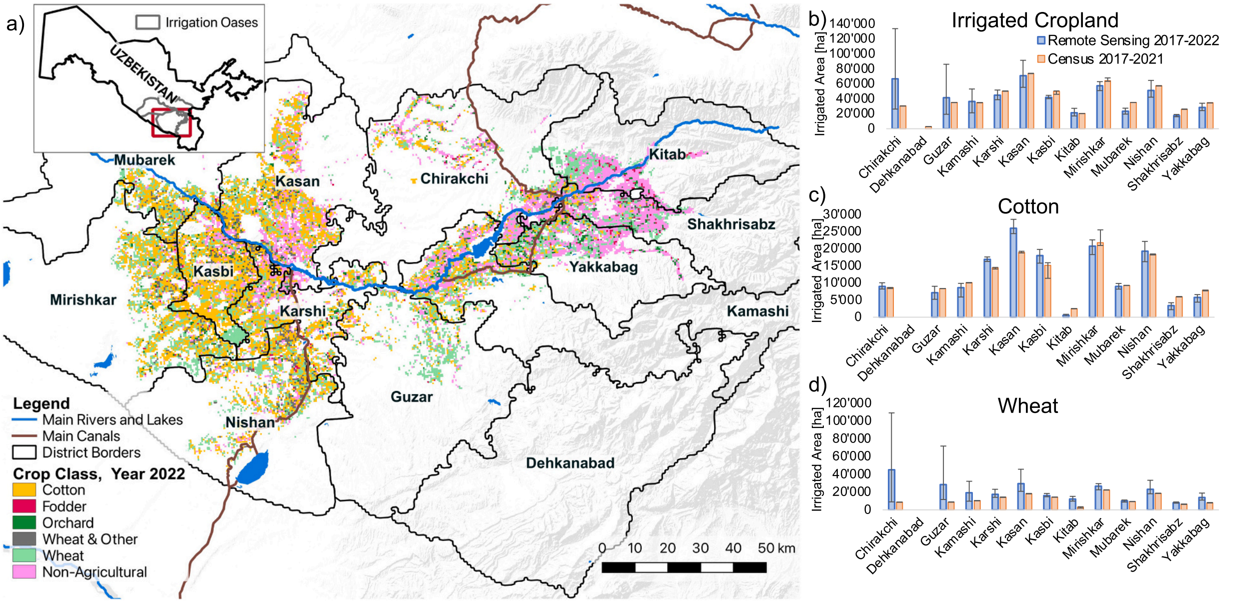

Fig. 7. a) Map of crop classes of the year 2022 and district boundaries of Kashkadarya Region. B) Validation of total irrigated cropland, c) cotton area, and d) wheat area as identified from remote sensing and compared with census data. The bars show the mean annual areas per district, and error bars represent the full range of annual values.

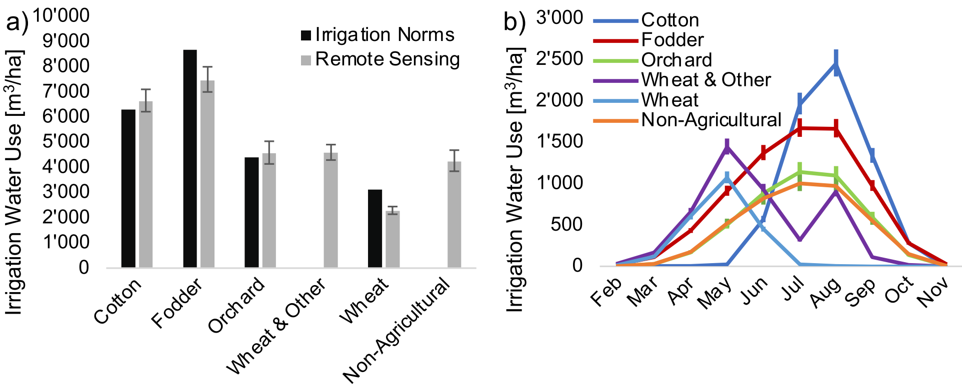

Fig. 8. a) Mean annual irrigation water use per crop class in Samarkand oasis according to irrigation norms and remote sensing (RS), respectively. For the classes 'Wheat & Other' and 'Non-Agricultural' the irrigation norms are not available. b) Mean monthly irrigation water use in Samarkand oasis based on the remote sensing analysis. Irrigation water use according to RS is calculated as crop irrigation water use (denoted as ETblue in Eq. 2) divided by field efficiency. Error bars show the uncertainty in RS-derived values, attributed to parameter uncertainty (Table 1).

(Khaydar et al., 2021). The unique hydrological conditions in Central Asia, particularly the peak in river flow during summer months due to snow and glacier melt, align well with the irrigation requirements of cotton (Fig. 8b and Supplementary Figure A6). This synchronicity between the peak in river flows and the peak irrigation demand of cotton makes cotton a viable and common crop in the region, as it requires substantial water input during its peak growing period in the late summer.

4.5. *Off-season irrigation*

Off-season irrigation represents water used for carrying out soil leaching, moisture-recharging and cleaning the collector-drainage network. The official data available to this study shows that salt removal by leaching is especially common in Bukhara, whereas water charging is most frequently used in Kashkadarya region (Fig. 9a). High volumes used for water charging could be associated with larger areas used for wheat cultivation, as Kashkadarya oasis has the largest fraction of irrigated areas used for wheat cultivation (40 % considering both single and double crop patterns, see Fig. 6).

The reference data indicate the off-season irrigation is more important in Bukhara and Kashkadarya than in Samarkand (Fig. 9a). However, the data were collected 20 years prior to our study period, and it is questionable whether the reported differences between regions are still representative. The validation data on total drainage volumes from 2019 and 2020 suggests an opposite relationship between Bukhara and Samarkand (Fig. 9c), although the validation data here do not differentiate between on- and off-season irrigation drainage.

Our range of estimates for total drainage from Bukhara (2.61 ± 0.4 km^3/a) falls within the value reported by official data (2.4 km^3/a, Fig. 9c). In Samarkand, however, our estimates underestimate the official data by 36 % on average. The cause of this underestimation is unclear. Off-season drainage volume estimates depend on assumptions regarding drainage water re-use fractions (Supplementary Table A5), field losses and conveyance losses (Appendix B). However, even assuming 100 % drainage water re-use would not align our data with the official data in Samarkand. We would further have to assume that there are practically no conveyance losses, which is not a realistic assumption. It would also not be justified to assume much higher field losses in Samarkand than in Bukhara. One explanation for the higher-than-expected total drainage volume in Samarkand could be drainage from groundwater. Drainage from groundwater through the collector-drainage system could be more significant in Samarkand than in Bukhara. The elevation of irrigated areas in the Bukhara oasis varies from 190 to 300 m asl. over a span of 160 km. In contrast, the Samarkand oasis extends over an elevation range of 300–1100 m asl, with elevation differences of several hundred meters occurring within less than 10 km at the southeastern edge of the oasis. This significant variation in elevation in Samarkand likely results in a more substantial groundwater movement, driven by the steeper hydraulic gradient. This would also explain the discrepancies between the two reference datasets.

The distribution of total off-season irrigation as estimated by our model mirrors that of areas with water charging, with Kashkadarya having the highest off-season irrigation values (Fig. 9b). In terms of total off-season irrigation per hectare of irrigated area, the highest values are observed in Bukhara (3700 ± 460 m^3/ha), while the lowest are in Samarkand (1900 ± 1050 m^3/ha). Experimental data on soil leaching per hectare from Bukhara, as noted by Khamidov et al. (2020), indicate a soil leaching requirement of about 4620 m^3 /ha considering the traditional method, with 85.8 % of irrigated land being saline and needing cleaning. Averaged over all irrigated areas in Bukhara, this equates to an average leaching rate of 3960 m^3 per hectare of irrigated area, aligning closely with our findings.

According to our analysis, the proportion of off-season irrigation compared to on-season irrigation ranges from an average of 39 % in Samarkand, 46 % in Bukhara to 78 % in Kashkadarya. Regardless of parameter uncertainty and the representativeness of official data, all datasets consistently indicate that soils in the arid and hyper-arid regions of Uzbekistan such as the ZKRB are inherently demanding. They require intensive management to mitigate issues like soil salinization, which substantially increases the total irrigation water demand.

4.6. Groundwater use

The residuals in the monthly water balance attributed to groundwater contribution add up to 0.81 ± 0.38 km^3 per year in Bukhara, 0.5 ± 0.38 km^3 /a in Kashkadarya, and 0.96 ± 0.47 km^3 /a in Samarkand (Fig. 4, Supplementary Table A2). Up-to-date public information on regional groundwater use in Uzbekistan is not available. The latest available official estimates, provided by the State Committee for Nature Protection of the Republic of Uzbekistan, refer to the years 2002–2004 (Rakhmatullaev et al., 2012). According to these estimates, the annual groundwater withdrawal in Bukhara region was 0.29 km^3 , 0.69 km^3 in Kashkadarya, and 0.66 km^3 in Samarkand region. 0.19 km^3 were withdrawn in Navoi region, which partly overlaps with Bukhara and Samarkand oases (Fig. 1). In the entire region, this amounts to a total withdrawal of 1.83 km^3 per year. This number is only 20 % lower than our average estimate of total groundwater withdrawal within the three oases (2.3 km^3). However, in recent years groundwater exploitation in the region has increased (Gafurov et al., 2019) and precipitation, a major factor affecting groundwater storage (Hu et al., 2021), varies significantly annually (Hu et al., 2017). Hence, comparing groundwater use across different periods is of limited value due to these temporal

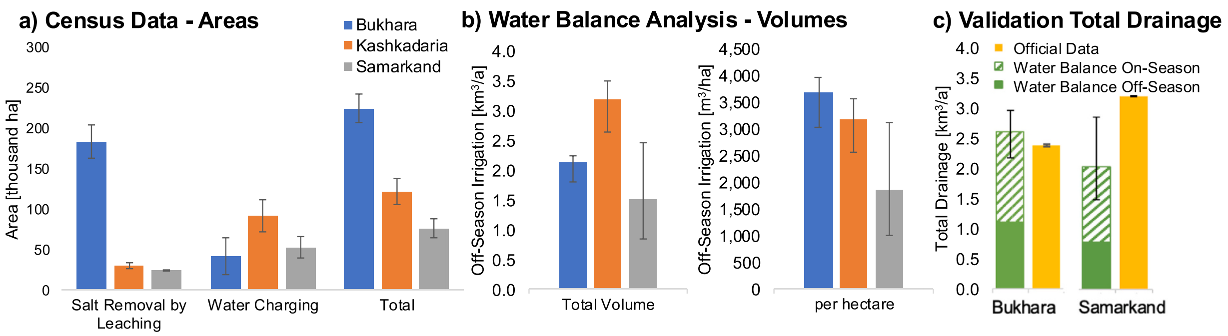

Fig. 9. a) Census data on off-season irrigation: areas treated by salt removal by leaching, water charging, and total area treaded by off-season irrigation, respectively. The data show the average of the two autumn-winter periods 1998–1999 and 2001–2002, and the full range of values. b) Water volumes used for off-season irrigation according to the water balance analysis: average total volumes of water used for off-season irrigation and average volume applied per hectare of irrigated area, respectively. c) Average annual drainage volume per irrigation oasis according to official data and according to the water balance approach, respectively. The error bars in b) and c) represent the full range of annual values in combination with the full range of parameter uncertainty.

variations and increasing exploitation.

Our estimates of annual groundwater use for 2017–2022 show considerable fluctuation, ranging from 1.15 km^3 to 3.5 km^3 (Fig. 10a). These fluctuations correlate with annual TWS depletion from GRACE satellite data, showing a strong relationship with a correlation coefficient of 0.82, and a coefficient of determination of the linear regression of 0.61 (Fig. 10b). The significant correlation (p-value < 0.05) underscores the reliability of our indirect method for estimating groundwater withdrawal, aligning closely with real-world data.

2018 was the only year where the average annual winter (November – April) TWS recharge exceeded the observed summer (April – November) TWS depletion (Fig. 10c), aligning with our lowest groundwater withdrawal estimate of 1.15 ± 0.76 km^3 for that year. By applying a linear regression to our groundwater use estimates and net TWS changes, considering observed annual TWS depletion and average annual winter TWS recharge, we determined an average sustainable groundwater withdrawal rate at 2.09 ± 0.94 km^3 /a (Fig. 10d). This value represents thus the maximum annual groundwater volume that can be sustainably used in a year with average TWS recharge during winter. This value was exceeded on average by 0.18 ± 0.04 km^3 /a, meaning that the groundwater withdrawal rate in the entire region needs to be reduced on average by at least 8.0 % ± 1.6 % to reach sustainability, according to our estimation. A volume of 0.18 km^3 /a accounts for just 25 % of the discrepancy between the originally designed and the currently used storage capacity of reservoirs in Kashkadarya (Section 4.2). This suggests that realizing even a small portion of the originally planned reservoir capacity could have a significant impact on reducing groundwater overuse. However, the absence of excess flows for filling additional reservoir storage clearly indicates that, unless current irrigation water use is reduced, replacing current groundwater use would lead to further reliance on pumped water resources.

In comparison to most other methods for groundwater withdrawal estimation discussed in recent review studies (Brookfield et al., 2024; Meza-Gastelum et al., 2022), the method presented in this study offers the advantage of being applicable to schemes with conjunctive use of surface water and groundwater for irrigation. It represents a viable alternative to volume-based methods in settings with limited availability of observational data. Furthermore, in comparison to previous studies that estimate groundwater pumping as closure to the water balance (Hunink et al., 2015; Isidoro et al., 2004; Ruud et al., 2004), our approach uniquely relies only on observations of river discharge, without the need for measurements of total surface water diversions for irrigation. We achieve water balance closure by interpreting data on reservoir storage changes, which, as demonstrated, can be accurately obtained from remote sensing.

4.7. *Limitations and future research*

Recent work by Hu et al. (2024) highlights the growing complexity and interdependence of water, food, energy, and carbon systems in Central Asia. Given the region's diversity institutional, socio-economic conditions, and agro-ecological settings, a geographically nuanced approach is essential for tailoring management strategies to local context (Kienzler et al., 2012). Legacy inefficiencies stemming from the Soviet era (O'Hara, 2000), combined with persistent tensions over transboundary water resources (Siegfried and Bernauer, 2025), further underscore the need for integrated, context-specific solutions.

By disaggregating agricultural water use, this study offers practical insights into local-scale dynamics that can support broader

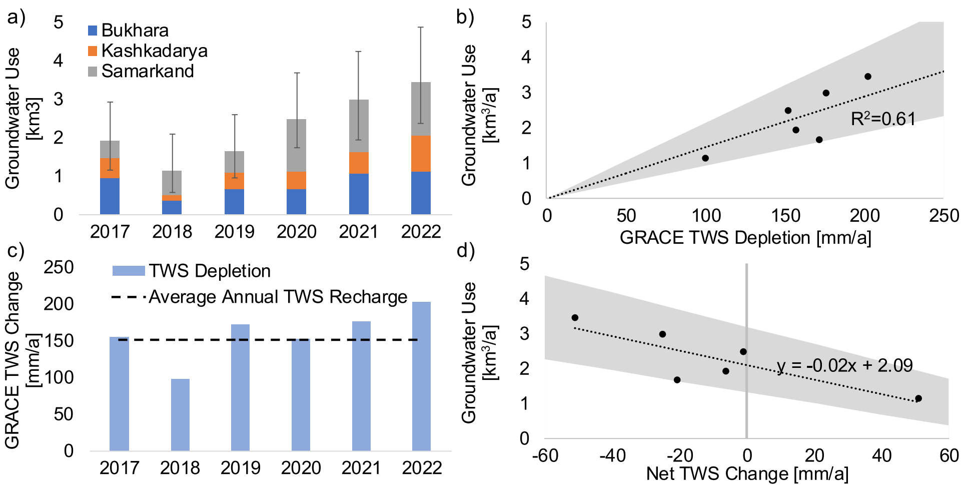

Fig. 10. Comparison of annual groundwater use as identified from the annual water balance analysis to GRACE annual terrestrial water storage (TWS) changes. a) Stacked annual groundwater use per irrigation oasis (units of km3 per year). b) Relationship between TWS Depletion and Groundwater Use. The R2 indicates the coefficient of determination of the linear regression function fitted to the annual data points. c) Annual TWS depletion and average annual winter (November-April) TWS recharge (units of mm per year). d) Relationship between groundwater use and net TWS changes, considering observed annual TWS Depletion and average annual TWS recharge. The equation of the fitted linear regression function is indicated, whereas the constant (2.09 km3/a) represents the estimated sustainable groundwater use in a year with an average TWS recharge. Error bars and shaded areas indicate the uncertainty in total annual groundwater use due to parameter uncertainty (Table 1).

regional coordination. These data help bridge the gap between water supply and demand across the region (Huang et al., 2022). Future research could build on this work by integrating high-resolution water use estimates with energy and carbon accounting frameworks, facilitating more holistic evaluations and informing the development of nexus-aligned agricultural policies.

Our findings also underscore a heavy reliance on pumped irrigation and indicate significant groundwater overdraft – patterns that reflect wider regional trends across Central Asia. While global groundwater storage data from GRACE satellites provide valuable macro-level insights, their coarse spatial resolution (>150,000 km^2) limits their utility for local-scale decision-making (Jasechko et al., 2024). This study addresses that limitation by quantifying annual groundwater use at the irrigation oasis level (~15,000 km^2), significantly improve spatial resolution and aligning more closely with local planning needs.

By isolating groundwater contributions within individual oases, we enable more accurate assessment of seasonal variability, groundwater dependence, and depletion risks. Future research could expand upon this by estimating sustainable withdrawal rates through the integration of groundwater table observations from wells, rather than relying solely on coarse TWS changes from GRACE.

Nevertheless, several limitations of this study must be acknowledged. First, our estimates of evapotranspiration and reservoir storage, derived from remote sensing, carry inherent uncertainties. Second, the study period (2017–2022) is relatively short and may not fully capture interannual climate variability or extreme hydrological events. Third, groundwater use was inferred as the residual of the water balance, which assumes all major fluxes are accurately measured. Unmonitored losses (e.g., infiltration losses from rivers) or systematic errors in other components may affect the precision of our groundwater abstraction estimates.

Improved calibration in using in-situ data and long-term validation is essential before this methodology can be fully adopted into water allocation planning, drought preparedness strategies, or agricultural accounting systems. Lastly, this analysis is limited to three oases in a single region, which may constrain the broader applicability of findings without further adaptation to different hydrogeological and governance settings across Central Asia. Recognizing these limitations provides an important context for interpreting our results and identifies key areas for future research aimed at enhancing the sustainability and resilience of water management systems in the region.

5. Conclusions

This study introduces advanced remote sensing methods for quantifying and monitoring water use in large, data-limited irrigation oases. By utilizing earth observation data, we enhanced the estimation of key hydrological components, particularly reservoir storage and irrigation water use. We demonstrate how optical remote sensing imagery, combined with satellite laser altimetry, can track the availability and use of active water storage in reservoirs. This approach allows for independent monitoring of active reservoir storage without relying on ground-based measurements or empirical VA-scaling, offering scalability to arid and semi-arid regions with similar data challenges. We show how this method can quantify the role of seasonal reservoir storage in meeting high water demands during peak irrigation periods.

In our study region, however, the dependency of agricultural productivity on water available from storage is lessened by utilizing groundwater for irrigation and pumping river water from the Amu Darya. Our analysis reveals that groundwater withdrawals play a crucial role in sustaining irrigation during surface water shortages but pose a risk of long-term resource depletion. Additionally, the energy-intensive process of river water pumping significantly contributes to the region's carbon footprint, emphasizing the need for improved groundwater management and more energy-efficient irrigation practices.

Our remote sensing estimates of actual evapotranspiration reveal that cotton has the highest irrigation water demand among the three studied oases. The peak water demand for cotton (July-August) coincides with the peak river flow, which is primarily fed by glacier and snowmelt. However, in Bukhara, cotton irrigation already exceeds the available water from Zarafshan River by 25 %. Adjusting water allocation policies could significantly enhance the sustainability of irrigation practices in the region. Our findings suggest that a shift to crops with different seasonal water demand would require adaptive reservoir management strategies. By systematically integrating Earth Observation data into a water balance analysis, this study provides a replicable framework for local water authorities to optimize regional water allocation and adjust reservoir operations accordingly.

Code availability

The code used in this study for generating reservoir bathymetry and reservoir volume time-series is openly available from https://doi.org/10.5281/zenodo.14979465 (Ragettli and Kreiner 2025).

CRediT authorship contribution statement

Siegfried Tobias: Writing – review & editing, Supervision, Project administration, Funding acquisition, Conceptualization. **Ragettli Silvan:** Writing – review & editing, Writing – original draft, Visualization, Software, Methodology, Investigation, Formal analysis, Data curation, Conceptualization. **Kreiner Adrian:** Writing – review & editing, Writing – original draft, Visualization, Investigation, Formal analysis, Data curation. **Yakovlev Andrey:** Validation, Resources, Data curation. **Anarbekov Oyture:** Validation, Resources. **Al-Zu'bi Maha:** Writing – review & editing, Resources. **Urazkeldiyev Abdikhamid:** Resources.

Declaration of Competing Interest

The authors declare that they have no known competing financial interests or personal relationships that could have appeared to influence the work reported in this paper.

Acknowledgments

This work has received funding from the Swiss Agency for Development and Cooperation under project 7F-10797.01.52. Reservoir level and volume data were obtained for Kashkadarya Oasis via the CGIAR Regional Initiative on Fragility to Resilience in Central and West Asia and North Africa (F2R-CWANA) and the CGIAR Scaling for Impact Program.

Appendix A. Supporting information

Supplementary data associated with this article can be found in the online version at doi:10.1016/j.ejrh.2025.102414.

Data availability

Data will be made available on request.

References

Abdullaev, I., 2004. The analysis of water management in bukhara oasis of Uzbekistan: historical and territorial trends. Water Int. 29 (1), 20–26. https://doi.org/10.1080/02508060408691744.

ADB. (2016). Tashkent Province Water Supply Development Project. In Asian Development Bank. ⟨https://www.adb.org/projects/46135-004/main⟩.

Aleksandrova, M., Lamers, J.P.A., Martius, C., Tischbein, B., 2014. Rural vulnerability to environmental change in the irrigated lowlands of Central Asia and options for policy-makers: a review. Environ. Sci. Policy 41, 77–88. https://doi.org/10.1016/j.envsci.2014.03.001.

Armon, M., Dente, E., Shmilovitz, Y., Mushkin, A., Cohen, T.J., Morin, E., Enzel, Y., 2020. Determining bathymetry of shallow and ephemeral desert lakes using satellite imagery and altimetry. Geophys. Res. Lett. 47 (7), 1–9. https://doi.org/10.1029/2020GL087367.

Awan, U.K., Anwar, A., Ahmad, W., Hafeez, M., 2016. A methodology to estimate equity of canal water and groundwater use at different spatial and temporal scales: a geo-informatics approach. Environ. Earth Sci. 75 (5), 409. https://doi.org/10.1007/s12665-015-4976-4.

Bekchanov, M., 2024. Conveyance efficiency and irrigation water productivity under varying water supply conditions in arid lowlands of Central Asia. Agric. Water Manag. 293, 108697. https://doi.org/10.1016/j.agwat.2024.108697.

Bekchanov, M., Bhaduri, A., Lenzen, M., Lamers, J.P.A., 2014. Integrating Input-Output Modeling with Multi-criteria Analysis to Assess Options for Sustainable Economic Transformation: The Case of Uzbekistan. In: Bhaduri, A., Bogardi, J., Leentvaar, J., Marx, S. (Eds.), The Global Water System in the Anthropocene: Challenges for Science and Governance. Springer International Publishing, pp. 229–245. https://doi.org/10.1007/978-3-319-07548-8_16.

Bekchanov, M., Lamers, J.P.A., Martius, C., 2010. Pros and cons of adopting water-wise approaches in the lower reaches of the amu darya: a socio-economic view. Article 2 Water 2 (2). https://doi.org/10.3390/w2020200.

Bekchanov, M., Ringler, C., Bhaduri, A., Jeuland, M., 2016. Optimizing irrigation efficiency improvements in the Aral Sea Basin. Water Resour. Econ. 13, 30–45. https://doi.org/10.1016/j.wre.2015.08.003.

Biemans, H., Haddeland, I., Kabat, P., Ludwig, F., Hutjes, R.W.A., Heinke, J., Von Bloh, W., Gerten, D., 2011. Impact of reservoirs on river discharge and irrigation water supply during the 20th century. Water Resour. Res. 47 (3), 2009WR008929. https://doi.org/10.1029/2009WR008929.

Brombacher, J., Silva, I.R.D.O., Degen, J., Pelgrum, H., 2022. A novel evapotranspiration based irrigation quantification method using the hydrological similar pixels algorithm. Agric. Water Manag. 267, 107602. https://doi.org/10.1016/j.agwat.2022.107602.

Brookfield, A.E., Zipper, S., Kendall, A.D., Ajami, H., Deines, J.M., 2024. Estimating groundwater pumping for irrigation: a method comparison. Groundwater 62 (1), 15–33. https://doi.org/10.1111/gwat.13336.

Buchhorn, M., Lesiv, M., Tsendbazar, N.-E., Herold, M., Bertels, L., Smets, B., 2020. Copernicus global land cover layers—collection 2. Remote Sens. 12 (6), 1044. https://doi.org/10.3390/rs12061044.

Cai, X., Feng, L., Hou, X., Chen, X., 2016. Remote sensing of the water storage dynamics of large lakes and reservoirs in the Yangtze River Basin from 2000 to 2014. Article 1 Sci. Rep. 6 (1). https://doi.org/10.1038/srep36405.

Che, X., Feng, M., Sexton, J., Channan, S., Sun, Q., Ying, Q., Liu, J., Wang, Y., 2019. Landsat-based estimation of seasonal water cover and change in arid and semi-arid central Asia (2000–2015). Remote Sens. 11 (11), 1323. https://doi.org/10.3390/rs11111323.

Cohen, J., 1960. A coefficient of agreement for nominal scales. Educ. Psychol. Meas. 20 (1), 37–46. https://doi.org/10.1177/001316446002000104.

Conrad, C., Dech, S.W., Hafeez, M., Lamers, J.P.A., Tischbein, B., 2013. Remote sensing and hydrological measurement based irrigation performance assessments in the upper Amu Darya Delta, Central Asia. Phys. Chem. Earth Parts ABC. 61–62, 52–62. https://doi.org/10.1016/j.pce.2013.05.002.

Conrad, C., Usman, M., Morper-Busch, L., Schönbrodt-Stitt, S., 2020. Remote sensing-based assessments of land use, soil and vegetation status, crop production and water use in irrigation systems of the Aral Sea Basin. A review. Water Secur. 11, 100078. https://doi.org/10.1016/j.wasec.2020.100078.

Cunha, H., Loureiro, D., Sousa, G., Covas, D., Alegre, H., 2019. A comprehensive water balance methodology for collective irrigation systems. Agric. Water Manag. 223, 105660. https://doi.org/10.1016/j.agwat.2019.05.044.

Djumaboev, K., Hamidov, A., Anarbekov, O., Gafurov, Z., Tussupova, K., 2017. Impact of institutional change on irrigation management: a case study from Southern Uzbekistan. Water 9 (6), 419. https://doi.org/10.3390/w9060419.

Djumaboev, K., Yuldashev, T., Holmatov, B., Gafurov, Z., 2019. Assessing water use, energy use and carbon emissions in lift- irrigated areas: a case study from karshi steppe in Uzbekistan. Irrig. Drain. 68 (3), 409–419. https://doi.org/10.1002/ird.2321.

Donchyts, G., Schellekens, J., Winsemius, H., Eisemann, E., Giesen, N. van de, 2016. A 30 m resolution surfacewater mask including estimation of positional and thematic differences using landsat 8, SRTM and OPenStreetMap: a case study in the murray-darling basin, Australia. Remote Sens. 8 (5). https://doi.org/10.3390/rs8050386.

Donchyts, G., Winsemius, H., Baart, F., Dahm, R., Schellekens, J., Gorelick, N., Iceland, C., Schmeier, S., 2022. High-resolution surface water dynamics in Earth's small and medium-sized reservoirs. Article 1 Sci. Rep. 12 (1). https://doi.org/10.1038/s41598-022-17074-6.

Eekelen, M.W. van, Bastiaanssen, W.G.M., Jarmain, C., Jackson, B., Ferreira, F., Zaag, P. van der, Okello, A.S., Bosch, J., Dye, P., Bastidas-Obando, E., Dost, R.J.J., Luxemburg, W.M.J., 2015. A novel approach to estimate direct and indirect water withdrawals from satellite measurements: a case study from the Incomati basin. Agric. Ecosyst. Environ. 200, 126–142. https://doi.org/10.1016/j.agee.2014.10.023.

van Eekelen, M.W., Bastiaanssen, W.G.M., Jarmain, C., Jackson, B., Ferreira, F., van der Zaag, P., Saraiva Okello, A., Bosch, J., Dye, P., Bastidas-Obando, E., Dost, R.J. J., Luxemburg, W.M.J., 2015. A novel approach to estimate direct and indirect water withdrawals from satellite measurements: a case study from the Incomati basin. Agric. Ecosyst. Environ. 200, 126–142. https://doi.org/10.1016/j.agee.2014.10.023.

FAO, 1989. Annex I: Irrigation efficiencies. In Irrigation Water Management: Irrigation Scheduling, https://www.fao.org/3/t7202e/t7202e08.htm.

Foley, D., Thenkabail, P., Oliphant, A., Aneece, I., Teluguntla, P., 2023. Crop water productivity from cloud-based landsat helps assess California's. Water Savings. Remote Sens. 15 (19), 4894, 10.3390/rs15194894.

Foody, G.M., 2002. Status of land cover classification accuracy assessment. Remote Sens. Environ. 80 (1), 185–201. https://doi.org/10.1016/S0034-4257(01)00295-4.

Foster, T., Mieno, T., Brozović, N., 2020. Satellite-based monitoring of irrigation water use: assessing measurement errors and their implications for agricultural water management policy. Water Resour. Res. 56 (11), e2020WR028378. https://doi.org/10.1029/2020WR028378.

Frenken, K., 2013. Irrigation in Central Asia in figures: AQUASTAT survey - 2012. FAO.

Fuentes, I., Vervoort, R.W., McPhee, J., Rojas, L.A.R., 2024. Agricultural water accounting: complementing a governance monitoring schema with remote sensing calculations at different scales. Agric. Water Manag. 292, 108676. https://doi.org/10.1016/j.agwat.2024.108676.

Funk, C., Peterson, P., Landsfeld, M., Pedreros, D., Verdin, J., Shukla, S., Husak, G., Rowland, J., Harrison, L., Hoell, A., Michaelsen, J., 2015. The climate hazards infrared precipitation with stations—a new environmental record for monitoring extremes. Sci. Data 2 (1), 150066. https://doi.org/10.1038/sdata.2015.66.

Gafurov, A., Selyuzhenok, V., Latinovic, M., Apel, H., Mamaraimov, A., Salokhiddinov, A., Boergens, E., Güntner, A., 2024. GRACE observes the natural and irrigation-induced regional redistribution of water storage in Central Asia. J. Hydrol.: Reg. Stud. 56, 101994. https://doi.org/10.1016/j.ejrh.2024.101994.

Gafurov, A., Yapiyev, V., Ahmed, M., Sagin, J., Haghighi, A.T., Akylbekova, A., Kløve, B., 2019. Chapter 3: Groundwater Resources in the Aral Sea Basin. In: Xenarios, S., Schmidt-Vogt, D., Qadir, M., Janusz-Pawletta, B., Abdullaev, I., Smakhtin, V. (Eds.), The Aral Sea Basin: Water for Sustainable Development in Central Asia. Routledge, p. 14.

Garcia, M., Ridolfi, E., Di Baldassarre, G., 2020. The interplay between reservoir storage and operating rules under evolving conditions. J. Hydrol. 590, 125270. https://doi.org/10.1016/j.jhydrol.2020.125270.

Glovatskii, O., Yangiev, A., Nasyrova, N., Gazaryan, A., Adjimuratov, D., Azizov, Sh, 2023. Results of field tests of the pumping station of the Karshi main Canal. AIP Conf. Proc. 2612 (1), 050024. https://doi.org/10.1063/5.0113299.

Glovatsky, O., Krutov, A., Ergashev, R., Gazaryan, A., Rashidov, J., Kholbutayev, B., 2023. Improv. Water intake Large Mach. Water uplifting Syst. Ex. Karshi Main. Canal 020031. https://doi.org/10.1063/5.0113298.

Grafton, R.Q., Williams, J., Perry, C.J., Molle, F., Ringler, C., Steduto, P., Udall, B., Wheeler, S.A., Wang, Y., Garrick, D., Allen, R.G., 2018. The paradox of irrigation efficiency. Science 361 (6404), 748–750. https://doi.org/10.1126/science.aat9314.

Groll, M., Opp, C., Kulmatov, R., Ikramova, M., Normatov, I., 2015b. Water quality, potential conflicts and solutions—An upstream–downstream analysis of the transnational Zarafshan River (Tajikistan, Uzbekistan). Environ. Earth Sci. 73 (2), 743–763. https://doi.org/10.1007/s12665-013-2988-5.

Groll, M., Opp, C., Kulmatov, R., Ikramova, M., Normatov, I., 2015a. Water quality, potential conflicts and solutions—An upstream–downstream analysis of the transnational Zarafshan River (Tajikistan, Uzbekistan). Environ. Earth Sci. 73 (2), 743–763. https://doi.org/10.1007/s12665-013-2988-5.

Hamidov, A., Helming, K., Balla, D., 2016. Impact of agricultural land use in Central Asia: a review. Agron. Sustain. Dev. 36 (1), 6. https://doi.org/10.1007/s13593-015-0337-7.

Hao, X., Fan, X., Zhao, Z., Zhang, J., 2023. Spatiotemporal patterns of evapotranspiration in central Asia from 2000 to 2020. Remote Sens. 15 (4), 1150. https://doi.org/10.3390/rs15041150.

Hashemy Shahdany, S.M., Firoozfar, A., Maestre, J.M., Mallakpour, I., Taghvaeian, S., Karimi, P., 2018. Operational performance improvements in irrigation canals to overcome groundwater overexploitation. Agric. Water Manag. 204, 234–246. https://doi.org/10.1016/j.agwat.2018.04.014.

Hu, Y., Duan, W., Zou, S., Chen, Y., De Maeyer, P., Van De Voorde, T., Takara, K., Kayumba, P.M., Kurban, A., Goethals, P.L.M., 2024. Coupling coordination analysis of the water-food-energy-carbon nexus for crop production in Central Asia. Appl. Energy 369, 123584. https://doi.org/10.1016/j.apenergy.2024.123584.

Hu, Z., Zhang, Z., Sang, Y.-F., Qian, J., Feng, W., Chen, X., Zhou, Q., 2021. Temporal and spatial variations in the terrestrial water storage across Central Asia based on multiple satellite datasets and global hydrological models. J. Hydrol. 596, 126013. https://doi.org/10.1016/j.jhydrol.2021.126013.

Hu, Z., Zhou, Q., Chen, X., Qian, C., Wang, S., Li, J., 2017. Variations and changes of annual precipitation in Central Asia over the last century. Int. J. Clim.

Hu, Z., Zhou, Q., Chen, X., Chen, D., Li, J., Guo, M., Yin, G., Duan, Z., 2019. Groundwater depletion estimated From GRACE: a challenge of sustainable development in an arid Region of Central Asia. Remote Sens. 11 (16), 1908. https://doi.org/10.3390/rs11161908.

Huang, W., Duan, W., Chen, Y., 2022. Unravelling lake water storage change in Central Asia: rapid decrease in tail-end lakes and increasing risks to water supply. J. Hydrol. 614, 128546. https://doi.org/10.1016/j.jhydrol.2022.128546.

Hunink, J.E., Contreras, S., Soto-García, M., Martin-Gorriz, B., Martinez-Álvarez, V., Baille, A., 2015. Estimating groundwater use patterns of perennial and seasonal crops in a Mediterranean irrigation scheme, using remote sensing. Agric. Water Manag. 162, 47–56. https://doi.org/10.1016/j.agwat.2015.08.003.

Ibrakhimov, M., Awan, U.K., George, B., Liaqat, U.W., 2018. Understanding surface water–groundwater interactions for managing large irrigation schemes in the multi-country Fergana valley, Central Asia. Agric. Water Manag. 201, 99–106. https://doi.org/10.1016/j.agwat.2018.01.016.

IEA, International Energy Agency. (2022). *Uzbekistan 2022 Energy Policy Review*. https://doi.org/10.1787/be7a357c-en.

Isidoro, D., Quílez, D., Aragüés, R., 2004. Water balance and irrigation performance analysis: La Violada irrigation district (Spain) as a case study. Agric. Water Manag. 64 (2), 123–142. https://doi.org/10.1016/S0378-3774(03)00196-3.

ISMITI. (2022). *Distribution of irrigated land in Samarkand region by hydromodule regions* [Dataset]. Scientific Research Institute of Irrigation and Water Problems under the Ministry of Water Resources of the Republic of Uzbekistan; Data provided by O. Anarbekov, International Water Management Institute (IWMI) Central Asia.

Jasechko, S., Seybold, H., Perrone, D., Fan, Y., Shamsudduha, M., Taylor, R.G., Fallatah, O., Kirchner, J.W., 2024. Rapid groundwater decline and some cases of recovery in aquifers globally. Nature 625 (7996), 715–721. https://doi.org/10.1038/s41586-023-06879-8.

Jasinski, M.F., Stoll, J.D., Hancock, D., Robbins, J., Nattala, J., Morison, J., Jones, B.M., Ondrusek, M.E., Pavelsky, T.M., Parrish, C., 2021. ATLAS/ICESat-2 L3A along track inland surface water data, Version 5. NASA Natl. Snow Ice Data Cent. Distrib. Act. Arch. Cent. https://doi.org/10.5067/ATLAS/ATL13.005.

Kamariddinovich, O.R., Rakhimjonovna, K.K., qizi, M.D.B., 2023. Improv. Methods Mapp. Irrig. Netw. Using GIS Technol. 11 (4), 691–699. https://doi.org/10.5281/zenodo.7823946.

Karimi, P., Bongani, B., Blatchford, M., Fraiture, C. de, 2019. Global satellite-based ET products for the local level irrigation management: an application of irrigation performance assessment in the Sugarbelt of Swaziland. Remote Sens. 11 (6). https://doi.org/10.3390/rs11060705.

Karimov, A.K., Toshev, R.H., Karshiev, R., Karimov, A.A., 2021. Water–energy nexus in Central Asia's lift irrigation schemes: multi-level linkages. Renew. Sustain. Energy Rev. 147, 111148. https://doi.org/10.1016/j.rser.2021.111148.

Khaidarov, A.R., 2020. Water use in Uzbekistan's segment of the zarafshan river: analytical review. Cent. Asian J. Water Res. 6 (2), 89–105. https://doi.org/10.29258/CAJWR/2020-R1.v6-2/89-105.eng.

Khamidov, M., Khamraev, K., Azizov, S., Akhmedjanova, G., 2020. Water saving technology for leaching salinity of irrigated lands: a case study from Bukhara region of Uzbekistan. J. Crit. Rev. 7 (02). https://doi.org/10.31838/jcr.07.01.99.

Khandelwal, A., Karpatne, A., Ravirathinam, P., Ghosh, R., Wei, Z., Dugan, H.A., Hanson, P.C., Kumar, V., 2022. ReaLSAT, a global dataset of reservoir and lake surface area variations. Sci. Data 9 (1), 356. https://doi.org/10.1038/s41597-022-01449-5.

Khaydar, D., Chen, X., Huang, Y., Ilkhom, M., Liu, T., Friday, O., Farkhod, A., Khusen, G., Gulkaiyr, O., 2021. Investigation of crop evapotranspiration and irrigation water requirement in the lower Amu Darya River Basin, Central Asia. J. Arid Land 13 (1), 23–39. https://doi.org/10.1007/s40333-021-0054-9.

Khazaei, B., Read, L.K., Casali, M., Sampson, K.M., Yates, D.N., 2022. GLOBathy, the global lakes bathymetry dataset. Sci. Data 9 (1), 36. https://doi.org/10.1038/s41597-022-01132-9.

Kienzler, K.M., Lamers, J.P.A., McDonald, A., Mirzabaev, A., Ibragimov, N., Egamberdiev, O., Ruzibaev, E., Akramkhanov, A., 2012. Conservation agriculture in Central Asia—What do we know and where do we go from here? Field Crops Res. 132, 95–105. https://doi.org/10.1016/j.fcr.2011.12.008.

Klein, I., Dietz, A.J., Gessner, U., Galayeva, A., Myrzakhmetov, A., Kuenzer, C., 2014. Evaluation of seasonal water body extents in Central Asia over the past 27 years derived from medium-resolution remote sensing data. Int. J. Appl. Earth Obs. Geoinf. 26, 335–349. https://doi.org/10.1016/j.jag.2013.08.004.

Landerer, F.W., Flechtner, F.M., Save, H., Webb, F.H., Bandikova, T., Bertiger, W.I., Bettadpur, S.V., Byun, S.H., Dahle, C., Dobslaw, H., Fahnestock, E., Harvey, N., Kang, Z., Kruizinga, G.L.H., Loomis, B.D., McCullough, C., Murböck, M., Nagel, P., Paik, M., Yuan, D., 2020. Extending the global mass change data record: GRACE follow-on instrument and science data performance. Geophys. Res. Lett. 47 (12), e2020GL088306. https://doi.org/10.1029/2020GL088306.

Landerer, F.W., Swenson, S.C., 2012. Accuracy of scaled GRACE terrestrial water storage estimates. Water Resour. Res. 48 (4), 2011WR011453. https://doi.org/10.1029/2011WR011453.

Li, Z., Fang, G., Chen, Y., Duan, W., Mukanov, Y., 2020. Agricultural water demands in Central Asia under 1.5C and 2.0C global warming. Agric. Water Manag. 231, 106020. https://doi.org/10.1016/j.agwat.2020.106020.

Liu, H., Chen, Y., Ye, Z., Li, Y., Zhang, Q., 2019. Recent lake area changes in central Asia. Sci. Rep. 9 (1), 1–11. https://doi.org/10.1038/s41598-019-52396-y.

Luo, Y., Zhang, Z., Zhang, L., Han, J., Cao, J., Zhang, J., 2022. Developing high-resolution crop maps for major crops in the european union based on transductive transfer learning and limited ground data. Remote Sens. 14 (8). https://doi.org/10.3390/rs14081809.

Markus, T., Neumann, T., Martino, A., Abdalati, W., Brunt, K., Csatho, B., Farrell, S., Fricker, H., Gardner, A., Harding, D., Jasinski, M., Kwok, R., Magruder, L., Lubin, D., Luthcke, S., Morison, J., Nelson, R., Neuenschwander, A., Palm, S., Zwally, J., 2017. The Ice, Cloud, and land Elevation Satellite-2 (ICESat-2): science requirements, concept, and implementation. Remote Sens. Environ. 190, 260–273. https://doi.org/10.1016/j.rse.2016.12.029.

Marti, B., Yakovlev, A., Karger, D.N., Ragettli, S., Zhumabaev, A., Wakil, A.W., Siegfried, T., 2023. CA-discharge: geo-located discharge time series for mountainous rivers in central Asia. Sci. Data 10 (1), 579. https://doi.org/10.1038/s41597-023-02474-8.

Mason, D.C., Davenport, I.J., Robinson, G.J., Flather, R.A., McCartney, B.S., 1995. Construction of an inter-tidal digital elevation model by the 'Water-Line' Method. Geophys. Res. Lett. 22 (23), 3187–3190. https://doi.org/10.1029/95GL03168.

Messager, M.L., Lehner, B., Grill, G., Nedeva, I., Schmitt, O., 2016. Estimating the volume and age of water stored in global lakes using a geo-statistical approach. Nat. Commun. 7 (1), 13603. https://doi.org/10.1038/ncomms13603.

Meza-Gastelum, M.A., Campos-Gaytán, J.R., Ramírez-Hernández, J., Herrera-Oliva, C.S., Villegas-León, J.J., Figueroa-Núñez, A., 2022. Review of groundwater withdrawal estimation methods. Water 14 (17), 2762. https://doi.org/10.3390/w14172762.

Mishra, B., Kumar, P., Saraswat, C., Chakraborty, S., Gautam, A., 2021. Water security in a changing environment: concept, challenges and solutions. Water 13 (4), 490. https://doi.org/10.3390/w13040490.

Msigwa, A., Komakech, H.C., Salvadore, E., Seyoum, S., Mul, M.L., van Griensven, A., 2021. Comparison of blue and green water fluxes for different land use classes in a semi-arid cultivated catchment using remote sensing. J. Hydrol.: Reg. Stud. 36, 100860. https://doi.org/10.1016/j.ejrh.2021.100860.

Muñoz-Sabater, J., Dutra, E., Agustí-Panareda, A., Albergel, C., Arduini, G., Balsamo, G., Boussetta, S., Choulga, M., Harrigan, S., Hersbach, H., Martens, B., Miralles, D.G., Piles, M., Rodríguez-Fernández, N.J., Zsoter, E., Buontempo, C., Thépaut, J.-N., 2021. ERA5-Land: a state-of-the-art global reanalysis dataset for land applications. Earth Syst. Sci. Data 13 (9), 4349–4383. https://doi.org/10.5194/essd-13-4349-2021.

Neuenschwander, A.L., Sheridan, R., Pitts, B.P., Jelley, J., Klotz, S.C., Popescu, R.F., Nelson, D., Harding, D., Pederson, Robbins, B., 2021. ATLAS/ICESat-2 L3A land and vegetation height. Version 5. NASA Natl. Snow Ice Data Cent. Distrib. Act. Arch. Cent. https://doi.org/10.5067/ATLAS/ATL08.005.

O'Hara, S., 2000. Lessons from the past: Water management in Central Asia. Water Policy 2 (4–5), 365–384. https://doi.org/10.1016/S1366-7017(00)00010-6.

Olsson, O., Gassmann, M., Manig, N., Ikramova, M., Wegerich, K., 2013. Basin efficiency approach and its effect on streamflow quality, Zerafshan River Uzbekistan. J. Hydrol. 476, 128–135. https://doi.org/10.1016/j.jhydrol.2012.10.022.

Olsson, O., Gassmann, M., Wegerich, K., Bauer, M., 2010. Identification of the effective water availability from streamflows in the Zerafshan river basin, Central Asia. J. Hydrol. 390 (3), 190–197. https://doi.org/10.1016/j.jhydrol.2010.06.042.

Pareeth, S., Karimi, P., 2023. Evapotranspiration estimation using Surface Energy Balance Model and medium resolution satellite data: an operational approach for continuous monitoring. Sci. Rep. 13 (1), 12026. https://doi.org/10.1038/s41598-023-38563-2.

Patle, P., Singh, P.K., Ahmad, I., Matsuno, Y., Leh, M., Ghosh, S., 2023. Spatio-temporal estimation of green and blue water consumptions and water and land productivity using satellite remote sensing datasets and WA+ framework: a case study of the Mahi Basin, India. Agric. Water Manag. 277, 108097. https://doi.org/10.1016/j.agwat.2022.108097.

Pettorelli, N., Vik, J.O., Mysterud, A., Gaillard, J.-M., Tucker, C.J., Stenseth, N.Chr, 2005. Using the satellite-derived NDVI to assess ecological responses to environmental change. Trends Ecol. Evol. 20 (9), 503–510. https://doi.org/10.1016/j.tree.2005.05.011.

Qadir, M., Noble, A.D., Qureshi, A.S., Gupta, R.K., Yuldashev, T., Karimov, A., 2009. Salt-induced land and water degradation in the Aral Sea basin: a challenge to sustainable agriculture in Central Asia. Nat. Resour. Forum 33 (2), 134–149. https://doi.org/10.1111/j.1477-8947.2009.01217.x.

Ragettli, S., Donauer, T., Molnar, P., Delnoije, R., Siegfried, T., 2022. Unraveling the hydrology and sediment balance of an ungauged lake in the Sudano-Sahelian region of West Africa using remote sensing. Earth Surf. Dyn. 10 (4), 797–815. https://doi.org/10.5194/esurf-10-797-2022.

Ragettli, S., Herberz, T., Siegfried, T., 2018. An unsupervised classification algorithm for multi-temporal irrigated area mapping in central Asia. Remote Sens. 10 (11), 1–23. https://doi.org/10.3390/RS10111823.

Ragettli, S., Kreiner, A., 2025. Remote sensing of active water storage in reservoirs and lakes. Comput. Softw. https://doi.org/10.5281/zenodo.14979465.

Rakhmatullaev, S., Huneau, F., Celle-Jeanton, H., Le Coustumer, P., Motelica-Heino, M., Masharif, B., 2013. Water reservoirs, irrigation and sedimentation in Central Asia: a first-cut assessment for Uzbekistan. Environ. Earth Sci. 68, 985–998. https://doi.org/10.1007/s12665-012-1802-0.

Rakhmatullaev, S., Huneau, F., Kazbekov, J., Celle-Jeanton, H., Motelica-Heino, M., Coustumer, P., Jumanov, J., 2012. Groundwater resources of Uzbekistan: an environmental and operational overview. Open Geosci. 4 (1), 67–80. https://doi.org/10.2478/s13533-011-0062-y.

Reddy, J.M., Jumaboev, K., Matyakubov, B., Eshmuratov, D., 2013. Evaluation of furrow irrigation practices in Fergana Valley of Uzbekistan. Agric. Water Manag. 117, 133–144. https://doi.org/10.1016/j.agwat.2012.11.004.

Remelgado, R., Zaitov, S., Kenjabaev, S., Stulina, G., Sultanov, M., Ibrakhimov, M., Akhmedov, M., Dukhovny, V., Conrad, C., 2020. A crop type dataset for consistent land cover classification in Central Asia. Sci. Data 7 (1), 1–6. https://doi.org/10.1038/s41597-020-00591-2.

Ruud, N., Harter, T., Naugle, A., 2004. Estimation of groundwater pumping as closure to the water balance of a semi-arid, irrigated agricultural basin. J. Hydrol. 297 (1–4), 51–73. https://doi.org/10.1016/j.jhydrol.2004.04.014.

Saidmamatov, O., Rudenko, I., Pfister, S., Koziel, J., 2020. Water–energy–food nexus framework for promoting regional integration in central Asia. Water 12 (7), 1896. https://doi.org/10.3390/w12071896.

Salameh, E., Frappart, F., Almar, R., Baptista, P., Heygster, G., Lubac, B., Raucoules, D., Almeida, L.P., Bergsma, E.W.J., Capo, S., Michele, M.D.D., Idier, D., Li, Z., Marieu, V., Poupardin, A., Silva, P.A., Turki, I., Laignel, B., 2019. Monitoring beach topography and nearshore bathymetry using spaceborne remote sensing: a review. Remote Sens. 11 (19). https://doi.org/10.3390/rs11192212.

Save, H., Bettadpur, S., Tapley, B.D., 2016. High-resolution CSR GRACE RL05 mascons. J. Geophys. Res.: Solid Earth 121 (10), 7547–7569. https://doi.org/10.1002/2016JB013007.

Scanlon, B.R., Fakhreddine, S., Rateb, A., de Graaf, I., Famiglietti, J., Gleeson, T., Grafton, R.Q., Jobbagy, E., Kebede, S., Kolusu, S.R., Konikow, L.F., Long, D., Mekonnen, M., Schmied, H.M., Mukherjee, A., MacDonald, A., Reedy, R.C., Shamsudduha, M., Simmons, C.T., Zheng, C., 2023. Global water resources and the role of groundwater in a resilient water future. Nat. Rev. Earth Environ. 4 (2), 87–101. https://doi.org/10.1038/s43017-022-00378-6.

Schmitt, R.J.P., Rosa, L., 2024. Dams for hydropower and irrigation: trends, challenges, and alternatives. Renew. Sustain. Energy Rev. 199, 114439. https://doi.org/10.1016/j.rser.2024.114439.

Schulz, S., Darehshouri, S., Hassanzadeh, E., Tajrishy, M., Schüth, C., 2020. Climate change or irrigated agriculture – what drives the water level decline of Lake Urmia. Sci. Rep. 10 (1), 1–10. https://doi.org/10.1038/s41598-019-57150-y.

Senay, G.B., 2018. Satellite psychrometric formulation of the operational simplified surface energy balance (SSEBop) model for quantifying and mapping evapotranspiration. Appl. Eng. Agric. 34 (3), 555–566. https://doi.org/10.13031/aea.12614.

Senay, G.B., Parrish, G.E.L., Schauer, M., Friedrichs, M., Khand, K., Boiko, O., Kagone, S., Dittmeier, R., Arab, S., Ji, L., 2023. Improving the operational simplified surface energy balance evapotranspiration model using the forcing and normalizing operation. Remote Sens. 15 (1), 260. https://doi.org/10.3390/rs15010260.

Sheffield, J., Wood, E.F., Pan, M., Beck, H., Coccia, G., Serrat-Capdevila, A., Verbist, K., 2018. Satellite remote sensing for water resources management: potential for supporting sustainable development in data-poor regions. Water Resour. Res. 54 (12), 9724–9758. https://doi.org/10.1029/2017WR022437.

Shi, C., Zhou, Y., Fan, X., Shao, W., 2013. A study on the annual runoff change and its relationship with water and soil conservation practices and climate change in the middle Yellow River basin. Catena 100, 31–41. https://doi.org/10.1016/j.catena.2012.08.007.

Siegfried, T., & Bernauer, T. (2025). International Water Problems in Central Asia Can Be Resolved Peacefully. Georgetown Journal of International Affairs (Under Review).

State Committee of the Republic of Uzbekistan, S. (2023). *Demography*. 〈https://stat.uz/en/official-statistics/demography〉.

Stringer, L.C., Mirzabaev, A., Benjaminsen, T.A., Harris, R.M.B., Jafari, M., Lissner, T.K., Stevens, N., Tirado-von Der Pahlen, C., 2021. Climate change impacts on water security in global drylands. One Earth 4 (6), 851–864. https://doi.org/10.1016/j.oneear.2021.05.010.

Taghvaeian, S., Neale, C.M.U., 2011. Water balance of irrigated areas: a remote sensing approach. Hydrol. Process. 25 (26), 4132–4141. https://doi.org/10.1002/hyp.8371.

Tatsumi, K., Yamashiki, Y., Torres, M.A.C., Taipe, C.L.R., 2015. Crop classification of upland fields using Random forest of time-series Landsat 7 ETM+ data. Comput. Electron. Agric. 115, 171–179. https://doi.org/10.1016/j.compag.2015.05.001.

Törnqvist, R., Jarsjö, J., 2012. Water savings through improved irrigation techniques: basin-scale quantification in semi-arid environments. Water Resour. Manag. 26 (4), 949–962. https://doi.org/10.1007/s11269-011-9819-9.

Varis, O., 2014. Resources: Curb vast water use in central Asia. Article 7520 Nature 514 (7520). https://doi.org/10.1038/514027a.

Velpuri, N.M., Senay, G.B., 2017. Partitioning evapotranspiration into green and blue water sources in the conterminous United States. Sci. Rep. 7 (1), 1–12. https://doi.org/10.1038/s41598-017-06359-w.

Wang, M., Chen, X., Sidike, A., Cao, L., DeMaeyer, P., Kurban, A., 2021. Optimal allocation of surface water resources at the provincial level in the Uzbekistan Region of the Amudarya River Basin. Water 13 (11), 1446. https://doi.org/10.3390/w13111446.

Xiong, J., Thenkabail, P.S., Gumma, M.K., Teluguntla, P., Poehnelt, J., Congalton, R.G., Yadav, K., Thau, D., 2017. Automated cropland mapping of continental Africa using Google earth engine cloud computing. ISPRS J. Photogramm. Remote Sens. 126, 225–244. https://doi.org/10.1016/j.isprsjprs.2017.01.019.

Xu, N., Ma, X., Ma, Y., Zhao, P., Yang, J., Wang, X.H., 2021. Deriving highly accurate shallow water bathymetry from sentinel-2 and ICESat-2 datasets by a multitemporal stacking method. IEEE J. Sel. Top. Appl. Earth Obs. Remote Sens. 14, 6677–6685. https://doi.org/10.1109/JSTARS.2021.3090792.

Xu, N., Xu, H., Wang, L., 2024. Deriving high-accuracy lake water-level changes from multi-source satellite datasets. Remote Sens. Lett. 15 (3), 302–312. https://doi.org/10.1080/2150704X.2024.2323555.

Yang, X., Wang, N., Liang, Q., Chen, A., Wu, Y., 2021. Impacts of human activities on the variations in terrestrial water storage of the Aral Sea Basin. Article 15 Remote Sens. 13 (15). https://doi.org/10.3390/rs13152923.

Yao, F., Livneh, B., Rajagopalan, B., Wang, J., Crétaux, J.-F., Wada, Y., Berge-Nguyen, M., 2023. Satellites reveal widespread decline in global lake water storage. Science 380 (6646), 743–749. https://doi.org/10.1126/science.abo2812.

Zanaga, D., Van De Kerchove, R., Daems, D., De Keersmaecker, W., Brockmann, C., Kirches, G., Wevers, J., Cartus, O., Santoro, M., Fritz, S., & others. (2022). *ESA WorldCover 10 m 2021 v200*. https://doi.org/10.5281/zenodo.7254220.

Zhang, K., Li, X., Zheng, D., Zhang, L., Zhu, G., 2022. Estimation of global irrigation water use by the integration of multiple satellite observations. Water Resour. Res. 58 (3), e2021WR030031. https://doi.org/10.1029/2021WR030031.